

AN EXPERIMENTAL INVESTIGATION OF THE
RHEOLOGICAL PROPERTIES OF VARIOUS POLYSTYRENE
COMPOSITES


By

James D. Small, Jr.

A DISSERTATION PRESENTED TO THE GRADUATE SCHOOL
OF THE UNIVERSITY OF FLORIDA IN PARTIAL FULFILLMENT
OF THE REQUIREMENTS FOR THE DEGREE OF
DOCTOR OF PHILOSOPHY

UNIVERSITY OF FLORIDA

1989



Digitized by the Internet Archive
in 2009 with funding from
University of Florida, George A. Smathers Libraries

Copyright 1989

by

James D. Small, Jr.

ACKNOWLEDGMENTS

The author wishes to thank Dr. A.L. Fricke for his guidance and friendship through the years required to obtain both the M.S. and Ph.D. degrees. His example of the work ethic, his character, and his friendship will always be an inspiration. He also wishes to thank Dr. G.A. Campbell of Clarkson University who "bailed" the author out when his first dissertation project proved unsuccessful after two years of work. His enthusiasm for the subject and his friendship are truly valued. The author would also like to thank Dr. C.L. Beatty whose enthusiasm and spirit helped the author through some extremely bad times during the course of this endeavor. He also wishes to express his appreciation to Dr. G. Hoflund and Dr. M.O. Balaban for their willingness to participate in the review and critique of this dissertation. The author considers himself most fortunate to not only be able to claim these gentlemen as his committee members, but to also be able to call them friends.

The author would also like to express his appreciation to Debbie Hitt, who prepared this manuscript, and to the Mobil Chemical Company and the employees of the Fabrication Laboratory, who on extremely short notice provided the necessary materials, processing equipment, and expertise to accomplish this research. Finally, the author wishes to express his gratitude to Miss JoEllen Kelly, the author's best friend and the colleague who obtained the capillary viscometric data, to Mary

Adams, who supplied the author with useful computer programs, and to Mark Davidson, Ron Baxley and Tracy Lambert, who assisted the author in solving the many electronic and mechanical problems that arose during this work. The author thanks you all.

TABLE OF CONTENTS

	<u>page</u>
ACKNOWLEDGMENTS	iii
LIST OF SYMBOLS	vii
LIST OF TABLES	x
LIST OF FIGURES	xi
ABSTRACT	xv
INTRODUCTION	1
PURPOSE OF INVESTIGATION	4
LITERATURE REVIEW	5
Newton's Law of Viscosity	5
Parallel Disk Rheometry	6
Melt Rheology of Polymer Composites	13
Percolation Theory	16
Rheological Models for Composite Systems	19
EXPERIMENTAL	24
Plan of Experimentation	24
Procedures	26
RESULTS	35
DISCUSSION OF RESULTS	83
Rheology of Filled Polystyrene	84
Effect of Concentration	85
Effect of Particle Size	86
Effect of Particle Size Distribution	87
Effect of Filler Type	88
Effect of Temperature	89
Cox-Merz Approximation	90
Rheological Models for Composite Systems	90
Phenomenological Interpretations	92
Limitations of Results	95
CONCLUSIONS	99

RECOMMENDATIONS	101
APPENDIX	103
REFERENCES	107
BIOGRAPHICAL SKETCH	111

LIST OF SYMBOLS

<u>Symbol</u>	<u>Definition</u>
A	Area, m^2
A_w	Filler specific surface area, m^2/g composite
a	Constant
E_a	Activation energy, kcal/mol
F	Force, N
G^*	Complex modulus, Pa
G'	Storage modulus, Pa
G''	Loss modulus, Pa
$G'_{R,0}$	Reduced storage modulus at zero frequency, Pa
H	Distance between parallel disks, mm
i	Index
N	Number of particles in a cluster
p_c	Critical concentration of occupied squares in statistical lattice
R	Disk radius, mm
r	Radial position
S	Power-law slope
T	Torque, N-m
t	Time, s
V	Velocity, m/s
v	Velocity profile
ω	Angular velocity, rad/s

x	Linear position
y	Linear position
Y	Distance between parallel plates, mm
γ	Strain
γ_o	Strain amplitude
$\dot{\gamma}$	Shear rate, s^{-1}
δ	Phase shift
λ	Relaxation time, s
θ	Circumferential position
ψ_1	Primary normal stress coefficient
ψ_2	Secondary normal stress coefficient
μ	Newtonian viscosity, Pa-s
$\ln \mu$	Adams model parameter
σ	Adams model parameter
η	Apparent viscosity, Pa-s
η^*	Complex viscosity, Pa-s
η'	Real component of η^* , Pa-s
η''	Imaginary component of η^* , Pa-s
η_o	Zero shear rate viscosity, Pa-s
η_o^*	Limiting frequency viscosity, Pa-s
η_R	Relative viscosity
ϕ	Filler volume fraction
ϕ_c	Critical filler volume fraction
ϕ_m	Maximum filler packing fraction
τ	Shear stress, Pa

τ_0 Shear stress amplitude, Pa
 ω Frequency, rad/s

LIST OF TABLES

<u>Table</u>		<u>page</u>
1	U.S. Consumption of Nonfibrous Extenders and Reinforcing Agents	2
2	Experimental Plan	25
3	Sample Identification Coding System	27
4	Extrusion Conditions Used to Compound the PS Composites	29
5	Actual Volume Fractions of CaCO_3 Filled Materials (Determining from ashing)	73
6	Actual Volume Fractions of Bimodally Distributed CaCO_3 Filled Materials (Determined from ashing) ..	74
7	The Activation Energy for the Onset of Viscous Flow for CaCO_3 Filled PS Materials	75
8	The Activation Energy for the Onset of Viscous Flow for Rubber Filled PS Materials	76
9	Viscosity Model Parameters for CaCO_3 Filled PS Materials	77
10	Viscosity Model Parameters for Rubber Filled PS Materials	78
11	Reduced Storage Modulus Model Parameters for CaCO_3 Filled PS Materials	79
12	Reduced Storage Modulus Model Parameters for Rubber Filled PS Materials	80
13	Intrinsic Viscosities of Selected PS Composites ..	81
14	Residual Water Adsorbed on CaCO_3 After Vacuum Drying (Determined by ashing)	82
15	Torque Calibration Data for RMS-800 with 2000 g-cm Transducer	96

LIST OF FIGURES

<u>Figure</u>		<u>page</u>
1	Steady Laminar Flow Between Parallel Plates	5
2	Steady Shear Flow in Parallel Disk Geometry	7
3	Dynamic Oscillatory Shear Flow in Parallel Disk Geometry	8
4	Square Lattice	17
5	The Effect of Nominal Concentration of 20 Micron CaCO ₃ on the Complex Viscosity of Polystyrene Composites at 210°C. Included are the Adams Model Predictions (___).	36
6	The Effect of Nominal Concentration of 2 Micron CaCO ₃ on the Complex Viscosity of Polystyrene Composites at 210°C. Included are the Adams Model Predictions (___).	37
7	The Effect of Nominal Concentration of 0.8 Micron CaCO ₃ on the Complex Viscosity of Polystyrene Composites at 210°C. Included are the Adams Model Predictions (___).	38
8	The Effect of Nominal Concentration of 1.9 Micron Rubber on the Complex Viscosity of Polystyrene Composites at 210°C. Included are the Adams Model Predictions (___).	39
9	The Effect of CaCO ₃ Particle Size Distribution on the Complex Viscosity of Polystyrene Composites at 210°C. Nominal Concentrations are 12 vol. %.	40
10	The Effect of CaCO ₃ Particle Size Distribution on the Complex Viscosity of Polystyrene Composites at 210°C. Nominal Concentrations are 20 vol. %. Included are the Adams Model Predictions for PS2020 (___) and PS202 (---).	41
11	The Effect of Nominal Concentration of 20 Micron CaCO ₃ on the Reduced Storage Modulus (G' / ω^2) of Polystyrene Composites at 210°C. Included are the Adams Model Predictions (___).	42

12	The Effect of Nominal Concentration of 2 Micron CaCO_3 on the Reduced Storage Modulus (G'/ω^2) of Polystyrene Composites at 210°C. Included are the Adams Model Predictions (____).	43
13	The Effect of Nominal Concentration of 0.8 Micron CaCO_3 on the Reduced Storage Modulus (G'/ω^2) of Polystyrene Composites at 210°C. Included are the Adams Model Predictions (____).	44
14	The Effect of Nominal Concentration of 1.9 Micron Rubber on the Reduced Storage Modulus (G'/ω^2) of Polystyrene Composites at 210°C. Included are the Adams Model Predictions (____).	45
15	The Effect of CaCO_3 Particle Size Distribution on the Reduced Storage Modulus (G'/ω^2) of Polystyrene Composites at 210°C. Nominal Concentrations 12 vol. %.	46
16	The Effect of CaCO_3 Particle Size Distribution on the Reduced Storage Modulus (G'/ω^2) of Polystyrene Composites at 210°C. Nominal Concentrations are 20 vol. %. Included are the Adams Model Predictions for PS2020 (---) and PS202 (____).	47
17	The Effect of Nominal Concentration of 20 Micron CaCO_3 on the Reduced Loss Modulus (G''/ω) of Polystyrene Composites at 210°C.	49
18	The Effect of Nominal Concentration of 2 Micron CaCO_3 on the Reduced Loss Modulus (G''/ω) of Polystyrene Composites at 210°C.	50
19	The Effect of Nominal Concentration of 0.8 Micron CaCO_3 on the Reduced Loss Modulus (G''/ω) of Polystyrene Composites at 210°C.	51
20	The Effect of Nominal Concentration of 1.9 Micron Rubber on the Reduced Loss Modulus (G''/ω) of Polystyrene Composites at 210°C.	52
21	The Effect of CaCO_3 Particle Size Distribution on the Reduced Loss Modulus (G''/ω) of Polystyrene Composites at 210°C. Nominal Concentrations are 12 vol. %.	53
22	The Effect of CaCO_3 Particle Size Distribution on the Reduced Loss Modulus (G''/ω) of Polystyrene Composites at 210°C. Nominal Concentrations are 20 vol. %.	54

23	The Effect of CaCO_3 Particle Size on the Complex Viscosity of Polystyrene Composites at 210°C. Nominal Concentrations are 10 vol. %.	55
24	The Effect of Both CaCO_3 and Rubber Particle Size on the Complex Viscosity of Polystyrene Composites at 210°C. Nominal Concentration are 25 vol. %. ...	56
25	The Effect of Concentration of 20 Micron CaCO_3 on the Reduced Viscosity (at limiting frequency) of Polystyrene Composites at 210°C. Included are the Campbell and Forgacs Model Predictions at $\phi_m = 0.74$ (---) and at $\phi_m = 0.524$ (___).	57
26	The Effect of Concentration of 2 Micron CaCO_3 on the Reduced Viscosity (at limiting frequency) of Polystyrene Composites at 210°C. Included are the Campbell and Forgacs Model Predictions at $\phi_m = 0.74$ (---) and at $\phi_m = 0.524$ (___).	58
27	The Effect of Concentration of 0.8 Micron CaCO_3 on the Reduced Viscosity (at limiting frequency) of Polystyrene Composites at 210°C. Included are the Campbell and Forgacs Model Predictions at $\phi_m = 0.74$ (---) and at $\phi_m = 0.524$ (___).	59
28	The Effect of Concentration of 1.9 Micron Rubber on the Reduced Viscosity (at limiting frequency) of Polystyrene Composites at 210°C. Included are the Campbell and Forgacs Model Predictions at $\phi_m = 0.74$ (---) and at $\phi_m = 0.524$ (___).	60
29	The Effect of Filler Specific Surface Area on the Reduced Viscosity (at limiting frequency as predicted by the Adams Model) of Polystyrene Composites at 210°C. Fillers are 2 Micron CaCO_3 (---) and 0.8 Micron CaCO_3 (___).	61
30	The Effect of Filler Specific Surface Area on the Adams Model Parameter, $\ln \mu$, for 2 Micron CaCO_3 (---) and 0.8 Micron CaCO_3 (___) Filled Polystyrene Composites at 210°C.	62
31	The Effect of Filler Specific Surface Area on the Adams Model Parameter, σ , for 2 Micron CaCO_3 (---) and 0.8 Micron CaCO_3 (___) Filled Polystyrene Composites at 210°C.	63
32	A Comparison of the Cox-Merz Approximation for PS2520 at 210°C. (Complex Viscosity = ___; Apparent Viscosity = ---).	64

33	A Comparison of the Cox-Merz Approximation for PS2508 at 210°C. (Complex Viscosity = ____; Apparent Viscosity = ---).	65
34	The Temperature Dependence of the Complex Viscosity of PS2520. (Temperatures in °C).	66
35	The Effect of Oxidative Degradation on the Complex Viscosity of Polystyrene at 210°C (____) and at 260°C (---).	67
36	The Effect of Oxidative Degradation on the Complex Viscosity of PS2020 at 210°C (____) and at 260°C (---).	68
37	SEM Micrographs of PS2520	69
38	SEM Micrographs of PS252	70
39	SEM Micrographs of PS2508	71

Abstract of Dissertation Presented to the Graduate School
of the University of Florida in Partial Fulfillment of the
Requirements for the Degree of Doctor of Philosophy

AN EXPERIMENTAL INVESTIGATION OF THE
RHEOLOGICAL PROPERTIES OF VARIOUS
POLYSTYRENE COMPOSITES

By

James D. Small, Jr.

May 1989

Chairman: Arthur L. Fricke

Major Department: Chemical Engineering

The understanding of the effects of the addition of a second phase into a polymer matrix on the melt rheological properties of the resulting composite system is of vital industrial importance. This investigation was initiated to provide the necessary experimental data to develop quantitative relationships between the melt flow properties of various polystyrene composites and the characteristic properties of the filled systems such as filler type, concentration, particle size and particle size distribution. Polystyrene-calcium carbonate and high impact polystyrene (rubber filled) were compounded using a commercially available polystyrene resin with a weight average molecular weight of 220,000 molecular weight units. The average particle sizes of the calcium carbonate fillers were 0.8, 2.0, and 20 microns, and the average size of the rubber domains in the impact modified polystyrene was approximately 1.9 microns. The concentration of these fillers in the resulting composite was varied between 5 and 30 volume percent, and several composites containing bimodal filler distributions were also prepared.

Rheological testing was accomplished by using a Rheometrics Mechanical Spectrometer in dynamic oscillatory mode over a temperature range of 210-260°C in a nitrogen environment. Limited steady shear viscosity data were obtained by using the Rheometrics Mechanical Spectrometer in steady shear mode, and these results combined with reported results obtained by capillary rheometry proved the validity of the Cox-Merz approximation for most of the experimental systems over a range of frequencies or shear rate of 0.01 to 10,000 s⁻¹.

The viscoelastic properties were found to be strongly dependent on filler concentration, filler particle size and particle size distribution, filler type (i.e., rubber or calcium carbonate), frequency, and temperature. The total specific surface area of the filler was shown to significantly affect the flow properties, and in fact, only at values of the total filler specific surface area greater than 2.7 m²/g composite was the Cox-Merz approximation proved unreliable. A stochastic model for the viscosity of polymer melts was modified to represent filled systems and was able to predict viscoelastic results with excellent reproducibility.

Finally, percolation theory was found to be useful in semi-quantitatively describing the rheological behavior of the composite systems. The results suggest that the critical percolation concentration (that concentration where a macroscopic interconnected cluster of filler particles is formed) was between 15 and 20 volume percent as predicted by theory.

INTRODUCTION

The economic and efficient processing of polymer melts is of tremendous industrial importance. During 1987, total U.S. polymer resin consumption increased 9% and has surpassed the 50 billion pounds per year level (1). Remarkably, of the twenty-three specific resin categories tabulated in Modern Plastics (1), each shared in the record growth.

In the U.S. plastics industry, there is a growing trend toward the modification of polymers, through the incorporation of various additives, to improve physical properties and/or cost competitiveness. With the demand for many polymer resins approaching the current supply levels (1), inexpensive fillers and extenders are becoming increasingly important. The use of nonfibrous fillers and extenders is increasing at a rate of approximately 4.5% annually (2), and as can be seen in Table 1, carbonates (calcium carbonate, chalk, and limestone) currently comprise more than 70% of the market. Other common additives include such items as antioxidants, flame retardants, processing aids, reinforcing agents, and coloring pigments or concentrates. As new filled systems are being developed, the need for reliable rheological information increases. All of the major melt processing operations are strongly dependent on the rheological properties of the polymeric material being processed. The addition of fillers and additives can significantly change the flow properties of the resulting composite, and therefore the processing of these composite systems can vary drastically.

Table 1. U.S. Consumption of Nonfibrous Extenders and Reinforcing Agents

<u>Material</u>	Consumption, million lbs.		
	<u>1985</u>	<u>1986</u>	<u>1987</u>
Carbonates	2710	2820	2950
Kaolin	170	190	210
Mica	22	25	30
Microspheres	18	20	23
Minerals	380	400	415
Organics	190	190	198
Silica	95	100	105
Talc	142	150	160
Others	8	9	11
TOTAL	3735	3904	4102

Obviously, it is extremely important to understand how the addition of a second phase into a polymer matrix affects the subsequent rheological properties. As expected, the flow behavior of composites may be influenced by the type of filler (i.e., rigid versus elastic), concentration of the filler, filler shape (sphere versus fiber), degree of matrix-particle bonding and interaction, filler particle size and distribution, temperature, deformation rate, and a myriad of other factors. It is highly impractical to perform complete rheological testing on all possible combinations of resins and additives.

Thus this investigation was initiated to provide the necessary experimental data to develop quantitative relationships between the melt flow properties of various polystyrene (PS) composites and the characteristic properties of the filled systems such as filler type, concentration, particle size, and particle size distribution. The models developed should predict the viscoelastic data over a wide range of frequency and/or shear rate with reliability. A major objective of the modelling was to relate the model parameters to physical properties of the filled systems. It is hoped that, such a model can be easily and methodically adapted to fit a wide variety of filled systems.

It should be noted that this investigation is part of a joint program, between the University of Florida and Clarkson University, established to study the interactions between composite melt rheology, subsequent processing, and final part properties. The rheological testing is being accomplished at the University of Florida, and Clarkson University is responsible for the processing (extrusion and injection molding) studies to follow. Both universities are jointly investigating the solid molded part properties.

PURPOSE OF INVESTIGATION

Since as previously described, a comprehensive investigation of all of the factors that influence the rheological behavior of filled systems would be most unwieldy, the main objective of this investigation was to systematically and quantitatively determine the effects of filler type, concentration, particle size, and particle size distribution on the rheological properties of PS composites. Additionally, the effects of temperature and shear rate or frequency were to be determined. The results could be used to help interpret future processing experiments, to aid in the planning of future rheological studies, and to discern the utility of available rheological models and predictive equations.

The second major objective of this study was to use the results of the proposed experimental work to test the adaptability of new theoretically based correlations that correctly predict the frequency or shear rate dependence of the viscosity of polymer melts to filled polymer systems. Data from at least two different composite systems will be used to test the newly developed models. It is hoped that by basing the models on measurable polymer and filler parameters, it will be proved generally useful in predicting flow properties of composite systems.

LITERATURE REVIEW

Newton's Law of Viscosity

For steady laminar flow, consider the parallel plate system presented in Figure 1.

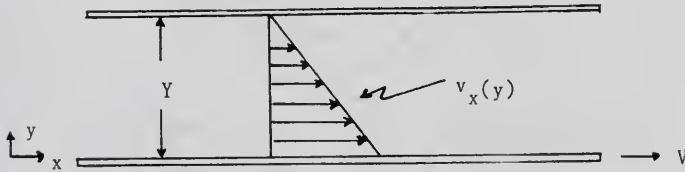


Figure 1. Steady Laminar Flow Between Parallel Plates

The lower plate moves in the x -direction at a constant velocity V , and at steady state the velocity profile, $v_x(y)$, is established. At steady state, a constant force F is required to maintain the motion of the lower plate and is expressed as

$$\frac{F}{A} = \mu \frac{V}{Y} \quad (1)$$

The proportionality constant μ is called the viscosity of the fluid. Equation (1) may be rewritten as

$$\tau_{yx} = -\mu \frac{dv_x}{dy} \quad (2)$$

where τ_{yx} is the shear stress exerted in the x-direction on a fluid in the region of lesser y, and v_x is the x-component of the fluid velocity vector. This is known as Newton's law of viscosity.

Parallel Disk Rheometry

The parallel disk rheometer is commonly used to study the viscometric functions of both polymeric and non-polymeric fluids. It is especially useful in the study of composites where the influence of the disks on the solid filler particles can be reduced by setting the gap between the disks such that it is much larger than the average filler particle size. The rheometer can usually be operated in either steady shear or dynamic oscillatory mode. Schematic representations of steady shear flow and oscillatory shear flow in the parallel disk geometry are shown in Figures 2 and 3, respectively.

Steady Shear Operation

During the steady shear operation of the parallel disk rheometer, the lower disk is rotated at a constant angular velocity W while the upper disk is held stationary. The assumptions used in the mathematical analysis of the parallel disk systems are

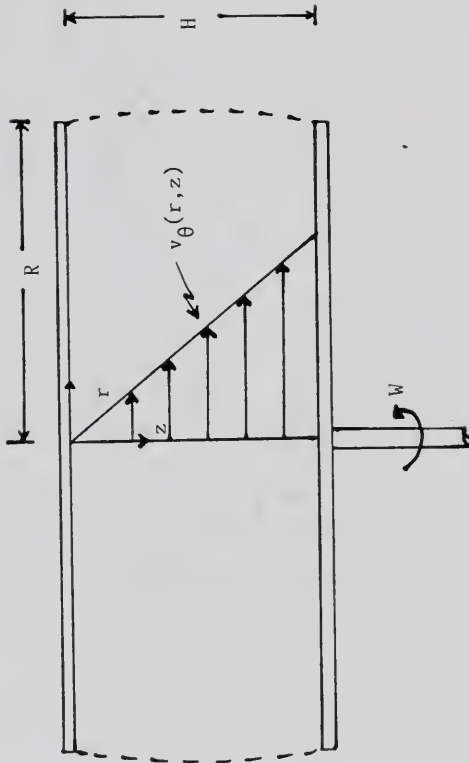


Figure 2. Steady Shear Flow in Parallel Disk Geometry

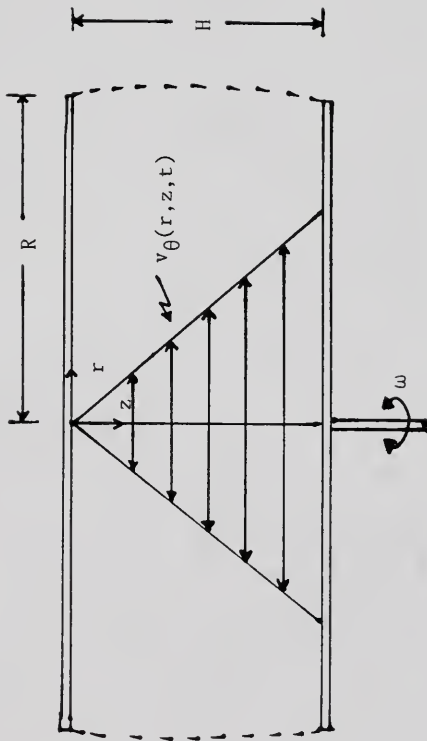


Figure 3. Dynamic Oscillatory Shear Flow in Parallel Disk Geometry

- (1) steady-state laminar flow
- (2) incompressible fluid
- (3) isothermal system (constant physical properties)
- (4) negligible inertial effects
- (5) no slip condition at the disk surface

With these assumptions, the equations of continuity and motion given by Bird et al. (3) can be solved to yield the fundamental equations for the system. The shear rate, $\dot{\gamma}_{z\theta}$, is a function only of radial position and is given by

$$\dot{\gamma}_{z\theta} = \frac{r\dot{W}}{H} \quad (3)$$

In order to determine the steady shear viscosity of the sample, the total torque required to maintain the stationary position of the upper disk must be measured. The total torque T can be expressed as

$$T = \int_0^{2\pi} \int_0^R (-r\tau_{z\theta}) r dr d\theta \quad (4)$$

The shear stress, $\tau_{z\theta}$, may be rewritten as

$$\tau_{z\theta} = - \eta \dot{\gamma}_{z\theta} \quad (5)$$

where η = apparent viscosity

and this expression may then be substituted into equation (4). However, because of the inhomogeneity of the shear field in the parallel disk

geometry, the apparent viscosity is not an explicit function of the applied torque as shown in equation (6)

$$T = 2\pi \int_0^R \eta \dot{\gamma} r^2 dr \quad (6)$$

Fortunately, by changing the variable of integration and by applying the Leibnitz rule for differentiation of a definite integral, the viscosity may be determined explicitly as a function of the shear rate and the applied torque by

$$\eta(\dot{\gamma}_R) = \frac{(T/2\pi R^3)}{\dot{\gamma}_R} \left[3 + \frac{d \ln(T/2\pi R^3)}{d \ln \dot{\gamma}_R} \right] \quad (7)$$

where $\dot{\gamma}_R$ is the shear rate at $r = R$.

The parallel disk rheometer can also be used to determine normal stresses that may be present in viscoelastic samples. The total force F that must be applied to maintain a constant gap between the disks has been shown by Bird et al. (3) to be related to the difference in primary and secondary normal stress coefficients, ψ_1 and ψ_2 respectively, as

$$\psi_1 - \psi_2 = \frac{1}{\dot{\gamma}_R^2} \left(\frac{F}{\pi R^2} \right) \left[2 + \frac{d \ln(F/\pi R^2)}{d \ln \dot{\gamma}_R} \right] \quad (8)$$

Dynamic Oscillatory Operation

In order to utilize the parallel disk rheometer to determine the unsteady response of a sample in small-amplitude oscillatory shear flow as shown in Figure 3, the bottom disk is oscillated sinusoidally with angular frequency ω , and the torque required to maintain the stationary position of the top disk is measured. This applied torque also varies

sinusoidally with frequency ω , but depending on the nature of the sample, it may or may not be in phase with the applied strain. The strain as a function of time is given by

$$\gamma = \gamma_0 \sin(\omega t) \quad (9)$$

where γ = sinusoidal strain

γ_0 = strain amplitude

t = time

If the strain amplitude is sufficiently small, the shear stress can be written as

$$\tau = \tau_0 \sin(\omega t + \delta) \quad (10)$$

where τ_0 = shear stress amplitude

δ = phase shift relative to the strain

Experimentally, the displacement of the bottom disk is proportional to the strain, and the torque is proportional to the stress, so the ratio of torque amplitude to displacement amplitude is equivalent to the ratio of stress amplitude to strain amplitude. The phase angle between the stress and strain is related to the response of the fluid. For a purely elastic material, $\delta = 0$, and the stress is in phase with the strain. For a purely viscous material, $\delta = 90^\circ$, and the stress lags the strain by 90° . Most materials are neither purely viscous nor purely elastic but are what is termed viscoelastic, and for these materials, $0 < \delta < 90^\circ$.

Using trigonometric identities and the stress strain phasors, the material functions can be calculated for a given frequency from

$$G' = (\tau_0/\gamma_0) \cos \delta \quad (11)$$

$$G'' = (\tau_0/\gamma_0) \sin \delta \quad (12)$$

The quantities G' and G'' are called the storage modulus and the loss modulus respectively. The storage modulus is related to the energy stored elastically in the material upon deformation, whereas the loss modulus represents the energy lost (converted to heat through molecular friction) due to viscous dissipation within the material.

The complex modulus G^* is defined as the magnitude of the vector sum of the in-phase and out-of-phase moduli:

$$G^* = |G^*| = [(G')^2 + (G'')^2]^{1/2} \quad (13)$$

The complex modulus gives an indication of the total energy required to deform a material.

The complex modulus and its components can be used to determine the complex viscosity η^* and its real and imaginary components, η' and η'' , respectively, as follows:

$$\eta^* = G^*/\omega \quad (14)$$

$$\eta' = G'/\omega \quad (15)$$

$$\eta'' = G'/\omega \quad (16)$$

It can be seen from equation (15) that the dynamic viscosity η' is proportional to the loss modulus, and thus η' also gives an indication of the energy dissipation that occurs during flow. Similarly, η'' is indicative of the energy stored by the fluid elastically upon deformation.

Melt Rheology of Polymer Composites

There exist in the literature many experimental studies involving the viscoelastic behavior of molten, amorphous polymer composites (4-45 e.g.). These investigations include a wide variety of thermoplastic resins in conjunction with both fibrous and non-fibrous fillers; however, there are numerous experimental discrepancies in the reported literature which make many of the results questionable. Common flaws in experimental procedures reported include the use of cone and plate geometries in obtaining rheological properties of filled systems, the assumption of negligible end effects in capillary rheometry, and the failure to report experimental errors in the measurements due to lack of replication, temperature control, and thermal stability of the composite sample. In all fairness, many of the assumptions used by previous investigators were employed to alleviate the costs associated with accounting for the possible problems.

Most of the work to date has focused mainly on the effect of filler concentration on the flow properties, while choosing to neglect the influence of the particle size and particle size distribution of the

solid phase. In fact, in a majority of the reported studies, only one filler particle size was actually investigated, thus eliminating any possibility of determining size effects. A few investigations are notable exceptions (12,13,14,15 and 27). Chapman and Lee (12) noted that the viscosity of talc filled polypropylene increased with increasing filler surface area; however, the two talc fillers used had equivalent average particle sizes and only slightly different particle size distributions. Kitano et al. (13) and Kataoka et al. (15) observed an increase in the reduced viscosity of polymers filled with smaller calcium carbonate particles, but their results were confounded by using different types of calcium carbonate with differing degrees of surface roughness. Kataoka et al. (14) investigated the effects of particle size of various types and sizes of glass fillers on the viscosity of both polyethylene and polystyrene composites. They noted that the melt rheological properties were strongly influenced by the glass concentration but were not appreciably affected by changes in the glass particle size. This may be attributed to the relatively larger filler particle sizes used in their work (> 30 microns). Suetsugu and White (27) observed increases in viscosity and yield stress with decreasing particle size for PS/CaCO₃ compounds at 30 vol. %; however, their emphasis in reporting centered on the yield phenomena in both steady shear and elongation. White and Crowder (45) observed that the melt viscosity increased dramatically as the filler particle size was decreased to less than 0.04 microns for various elastomers filled with carbon black. However, since surface adsorption of rubber on carbon black and covalent bonding between rubber and carbon black can occur in these systems, their results may not represent filled thermoplastic systems very well.

Equally scarce in the literature are detailed studies of the effects of filler particle size distribution on the rheology of polymer composites. Both Farris (35) and Chong et al. (30) observed that at concentrations greater than approximately 20 volume percent, the viscosities of suspensions of multimodal particle sizes were significantly lower than those of suspensions of unimodally dispersed particles at equivalent loading levels. It is worth noting that in these studies the concentration of smaller particles was always less than the concentration of the larger filler particles. There appear to be no data in the literature relating the effects of higher concentrations of smaller particles in multimodal systems, and the effects of particle size distribution on suspension viscosity in general are still neither well documented nor understood.

In almost all of the reported work, the composite or suspension viscosity increased with increased filler concentration over the entire shear rate or frequency range investigated. Also observed by many investigators was an increase in non-linear flow behavior with increasing solids loading, which resulted in shifting the point at which pseudoplasticity began to lower shear rates. Since the slopes of the flow curves in the fully developed power-law region were similar and relatively unchanged by change in filler concentration, the viscosity curves for different filler loadings, when superimposed, converged at higher deformation rates. Thus the viscosities in the limiting shear region showed much greater dependence on filler concentration than did the viscosities in the power-law region.

There are currently two predominant theories used to explain the observed influence of filler addition on the composite melt rheological

properties. Utracki and Fisa (4) and Kataoka et al. (15) have proposed that the increase in melt viscosity with increasing filler concentration may be attributed to an interfacial boundary layer of polymer associated with the filler particles. The mechanism assumes that the increase in viscosity may be attributed to an increase in apparent volume of filler attributed to the formation of a fixed layer of polymer on the filler surface. Kataoka et al. (15) have estimated that the thickness of the "fixed" polymer layer had to be at least 10% of the radius of the filler particle to account for deviations between experimental results and those predicted from various suspension models.

A second common explanation of the observed behavior previously discussed was attributed to the formation of structure in the form of a network within the filler domain (12). Agglomerating particles may form a network-like structure within the melt at low shear rates or frequencies, resulting in a large increase in relative viscosity. As the deformation rate increases, the network structure is destroyed, and the effect of filler content becomes negligible. The effect is a convergence of the flow curves for filled systems at high deformation rates.

Percolation Theory

Percolation theory involves the transition from random processes to processes where a macroscopic ordered structure develops. In order to explain percolation, consider the array of squares shown in Figure 4. Such an array, assumed to be sufficiently large so that effects from its boundaries are negligible, is usually called a square lattice (46). As seen in the figure, a certain fraction of the squares are occupied, and

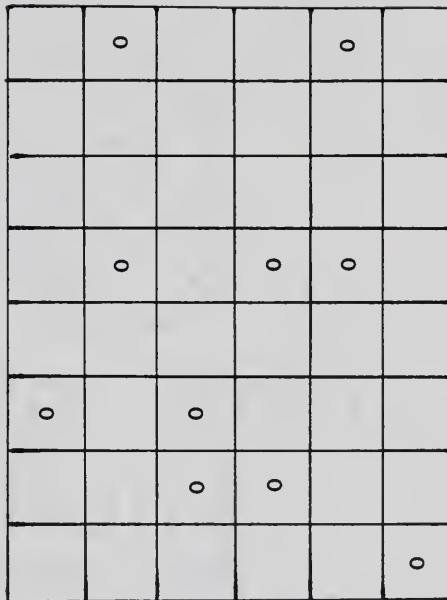


Figure 4. Square Lattice

the remainder are empty. Each of the occupied sites is filled randomly with a probability which is independent of neighboring sites. A cluster is defined as a group of occupied squares that share a common side, and it is the interest in the number and the properties of these clusters that constitutes percolation theory. At a critical concentration of occupied squares, p_c , the cluster percolates through the statistical system as a macroscopic connected entity, and the formation of this "infinite cluster" in real systems may have a dramatic effect on the physical properties of the system (47).

Percolation theory has been used to describe many diverse phenomena such as forest fires (48), diffusion in disordered media (49), and conductive properties of disordered systems (50). Historically, Flory (51) and Stockmayer (52) developed the theory of the Bethe lattice, which is now called percolation theory, to describe the gelation of macromolecules. This pioneering work led to the increased interest in percolation theory and its usefulness in describing critical phenomena.

The application of percolation theory to composite systems has focused mainly on the electrical transport phenomena in polymers filled with conducting fillers (50, 53, and 54). Conductive particles dispersed in insulating polymer matrices exhibit bulk conductivity above a critical concentration, while below the critical concentration, the materials are insulating. In general, the experimentally determined critical percolation concentrations are in good agreement with the theoretically and numerically determined value (50,55,56) of 16 volume percent.

No references regarding the use of percolation concepts to describe rheological properties of polymer composite systems were found, however

the dynamic viscosity of various microemulsion systems has been described by percolation processes (56,57 and 58). At increased concentration of the minor phase in emulsion systems, Stokes-Einstein predictions for reduced viscosity fail (57). However, the observed transitions at critical concentrations have been well predicted and described by percolation concepts. Two studies involving the application of percolation theory to describe the rheological behavior of concentrated suspensions were also discovered. Heyes (59) attributed the power-law dependence of the shear modulus with packing fraction, for computer simulated colloidal systems, to the onset of long range structural order in the system. Campbell and Forgacs (47) used percolation concepts to develop a stochastic model which predicted the limiting shear viscosity of a suspension as a function of filler concentration. Their model was used to predict slurry viscosities above the critical percolation concentration with excellent accuracy for several experimental systems.

Rheological Models for Composite Systems

Limiting Shear Viscosity

The development of rheological models to describe the effect of the addition of a second rigid phase to a fluid can be traced to the work of Einstein (60) who noted that the viscosity of Newtonian suspensions of rigid spheres was increased according to the following relationship:

$$\eta_R = 1 + 2.5 \phi \quad (17)$$

where η_R = relative viscosity

ϕ = volume fraction of spheres

Since Einstein's equation is based on only single particle interactions, its utility is restricted to very dilute systems (< 10 vol. %). Through the years the Einstein equation has been extended to account for the formation of multiple particle clusters (61 and 62), and in the resulting equations, the higher order terms represent the interactions of two or more particles. All of these equations are of the form

$$\eta_R = a_0 + \sum_{i=1}^N a_i \phi^i \quad (18)$$

where N = number of particles in the cluster formation

In these models, the total energy dissipated during flow is determined as a summation of the contributions from the particles and groups of particles similar to the method used by Einstein.

Since the early theoretical work, many empirical and semi-empirical models to predict the effect of particle concentration on slurry limiting shear viscosity have been developed. An extensive review of these developments was reported by Utracki and Fisa (4). Their results indicate that most of the proposed models predict, within reasonable limits, the increase in suspension viscosity with increase in concentration of the second phase at concentrations well beyond the limits imposed on the Einstein equation. However it should be noted that no matter how valid the physical assumptions that were used to develop the theoretical models of the form of equation (16), a power series equation would fit the data, provided enough terms were used. This fact is manifested in

the result that for many of the proposed models, the reduced viscosity does not approach infinity as the volume fraction of the rigid phase approaches 1. Finally, it should also be noted that the overwhelming majority of the work involving modelling of polymer composite systems has historically consisted of extrapolating the slurry results by modifying the available adjustable parameters without regard to the significant physical differences in the two systems.

A more broad ranging phenomenological approach was employed by Campbell and Forgacs (47) in their modelling work to determine the effects of concentration on concentrated suspension viscosity. Their approach involved the application of percolation theory to describe and quantify the effect the addition of a second phase has on suspension viscosity. The resulting stochastic equation

$$\eta_R = \exp\left(\frac{\phi_m - \phi_c}{\phi_m - \phi}\right) - 1 \quad (19)$$

where ϕ_m = maximum filler packing volume fraction

ϕ_c = critical volume fraction = 0.16

not only produced excellent prediction of available slurry data, but also allowed justifiable extrapolation to filled macromolecular systems since the concepts encompassed in percolation theory are not material dependent. The only adjustable parameter in equation (19) is ϕ_m which is determined from geometrical and probabilistic arguments. The critical percolation concentration is, to a very good approximation, independent of material properties and has the value of 0.16 (50,55 and 56).

Shear Rate Dependent Viscosity

There are in the literature a myriad of constitutive equations developed to describe the shear stress-shear rate behavior for pure polymer systems. These range in complexity from the simple power-law relationship to the eight constant Oldroyd model. An excellent review of available rheological models is found in Byrd et al. (3). These models are all based on continuum mechanics and are developed for homogeneous systems. Farrington (63) recently reviewed the general state of the art knowledge in molecularly based rheological models of homogeneous systems. Any of these models could be extended to heterophase systems, by simply correlating the various parameters with the experimental results for composite systems, to yield models whose parameters would then depend on properties related to the filled system (e.g., filler size and volume fraction). However, these models are quite unwieldy and so it seems much easier and somewhat more applicable to start with a model that lends itself to a clear simple extension to heterophase systems. Such a stochastic model was presented by Adams (64). In her model, the viscosity of a polymer is related to the numbers of molecules of given sizes in the system, with the higher molecular weight "solvent" molecules. Thus during flow at low shear rates, the higher molecular weight larger molecules can deform quickly enough to move segments into and out of available "holes" and therefore dissipate energy as molecular friction. As the shear rate increases, the largest molecules become trapped in certain configurations in the melt and cannot move into the available holes fast enough and therefore cannot dissipate energy as effectively. This phenomenon marks the onset of non-Newtonian flow. Further increases in shear rate entrap more and more molecules until in

the limit only "solvent" molecules can effectively dissipate energy. The result of her modelling effort was a predictive equation for the shear rate and molecular weight dependence of viscosity as follows:

$$\ln \eta_R = \frac{S\sigma}{\sqrt{2}} \left[\frac{\ln \mu - \ln \dot{\gamma}}{\sqrt{2}\sigma} \operatorname{erfc} \left(\frac{\ln \mu - \ln \dot{\gamma}}{\sqrt{2}\sigma} \right) - \frac{1}{\sqrt{\pi}} \exp \left(- \frac{(\ln \mu - \ln \dot{\gamma})^2}{2\sigma^2} \right) \right] \quad (20)$$

where S = negative slope in the fully developed power law region of the flow curve

σ and μ = model parameters

Equation (18) was obtained by twice integrating the negative log normal distribution function used to represent the viscosity-shear rate curve, and thus σ and μ are simply the distribution standard deviation and the distribution mean respectively. These parameters were then related to polymer properties such as molecular weight, polydispersity, and glass transition temperature. The resulting set of equations are easily manipulated (64).

Since this model has its foundation in structure formation, the percolation concepts previously discussed are applicable. Therefore it should be relatively easy to extend this model to composite systems, and by utilizing similar arguments as the original author, determine the effects of filler properties on the composite rheology.

EXPERIMENTAL

Plan of Experimentation

In order to efficiently determine the relationship between filler properties (type, concentration, particle size, and particle size distribution) and composite rheological properties, the experimental plan outlined in Table 2 was employed. The polymers used in this study were commercially available PS and high impact polystyrene (HIPS) with weight average molecular weights of approximately 220,000 molecular weight units. The impact modified PS was available with approximately 30 volume % of 1.8-2.0 micron rubber filler. The rigid CaCO_3 fillers employed were obtained from OMYA, Inc., and the pertinent physical properties and size distributions appear in Appendix I. The filler particles were neither chemically altered nor surface treated.

As shown in Table 2, the experimental plan was divided into three distinct groups, and the filler parameters (i.e., type, average particle size, and concentration) that were used to compound the PS composite samples are listed for each group. Results from the Group 1 samples provided information elucidating the effects of filler particle size and concentration on the composite viscoelastic properties. The Group 2 results were used to compare elastic and rigid fillers over broad ranges of particle size and concentration, whereas the Group 3 samples were used to test the effects of bimodal particle size distributions.

Table 2. Experimental Plan

<u>Filler Type</u>	<u>Average Particle Size, Microns</u>	<u>Nominal Filler Concentration, Volume %</u>	<u>Temperature, °C</u>
Group 1: CaCO ₃	. 20 2 0.8	5	
		10	210
		15	235
		20	260
		25	
Group 2: Rubber	1.9	6	
		12	210
		18	235
		24	260
		30.	
Group 3:	20 2		210
		12*	235
		20*	260

*Concentrations of 80/20, 60/40, 50/50, 40/60, 20/80.
Ratios of 20/2 micron filler.

The rheological properties of the samples comprising the experimental plan were determined by using a Rheometrics RMS-800 mechanical spectrometer, in both steady shear and dynamic oscillatory modes, since the instrument allowed precise control of both sample temperature and environment. The parallel plate geometry was employed throughout this investigation so that the influence of viscometer tooling on the rigid phase of the heterophase systems studied (i.e., "wall effects") was minimized.

Procedures

Sample Identification

A coding was developed to simplify references to the specific samples that were previously outlined in the experimental plan. The sample identification procedure appears in Table 3, and this coding was used throughout the remainder of this dissertation.

Preparation of Composite Samples

The various PS composite samples used in this study were prepared with the assistance of the Research and Development department of the Mobil Chemical Company in Edison, New Jersey. Polystyrene resin was combined with each of the three different size CaCO_3 fillers by mixing the materials in a 25 lb. capacity Stewart-Bolling Banbury mixer. The resulting masterbatches, PS2520, PS252 and PS1508, were then diluted with pure polymer to achieve the necessary composition. It should be noted that for the PS filled with 0.8 micron CaCO_3 , the maximum filler concentration that could be processed using the Banbury mixer was 15

Table 3. Sample Identification Coding System

Groups 1 and 2

<u>Coding:</u>	<u>Resin Material</u>	<u>Nominal Total Filler Concentration</u>	<u>Average Filler Particle Size</u>
exs.	PS2508:	Polystyrene filled with 25 vol. % of 0.8 micron CaCO_3	
	HIPS1000:	High impact PS filled with 10 vol. % rubber	

Group 3

<u>Coding:</u>	<u>Resin Material</u>	<u>Nominal Total Filler Concentration</u>	<u>Weight % of Total that is 20 micron filler</u>	<u>Weight % of Total that is 2 micron filler</u>
ex.	PS122080:	Polystyrene filled with 12 vol. % total filler. 20% of the CaCO_3 is 20 micron and 80% is 2 micron.		

vol. %, therefore PS2008 and PS2508 were compounded using a heated Farrel roll mill. The roll mill consisted of twin 12 in. circumference rolls heated with hot oil to temperatures of 235°F (front) and 225°F (rear) respectively. The front roll was rotated at a rate of 22 ft/min, and the rear roll was rotated at 27 ft/min.

Dilution and mixing of master batches to form the experimental samples outlined previously in Table 2, was accomplished by first mixing the materials to be compounded in a portable cement mixer and then by melt extruding the materials in a Werner-Pfleiderer ZSK50 corotating 30 mm twin screw extruder. The extrusion parameters used to accomplish the sample compounding are given in Table 4. The extruded strands were quenched in a water filled take-up trough and then fed to a pelletizer. The resulting composite pellets were then remixed in the cement mixer and reextruded, as before, to provide sufficient mixing. The HIPS composites were prepared similarly by using the commercially available HIPS 3000 as the masterbatch.

Test Sample Preparation

The samples used to perform the rheological testing were prepared by compression molding the individual composite samples using a Pasadena Hydraulic Inc. model SPW225C press with electrically heated platens. The composite pellets were first dried in a vacuum oven at 80°C for at least 8 hours to remove any residual moisture. The dried pellets were then poured into a 6" x 6" x 1/8" picture frame mold supported by a steel plate covered with teflon coated aluminum foil to prevent adhesion, and the plate and mold were placed onto the lower of the two preheated press platens. The temperature of the platens was maintained

Table 4. Extrusion Conditions Used to Compound the PS Composites

<u>Torque, % (125% max.)</u>	<u>Screw Speed, rpm</u>	<u>Feed Rate Set Point (10 max.)</u>	<u>Melt Pressure psig</u>	<u>Melt Temperature °F</u>
42-62	300	2.9-5.9	125-375	406-418

Barrel Temperature Profile					
<u>Zone #1</u>	<u>Zone #2</u>	<u>Zone #3</u>	<u>Zone #4</u>	<u>Zone #5</u>	<u>Zone #6</u>
160-195	260-305	365-400	400-405	400	400

at approximately 200°C. After the pellets had melted (approximately 15 minutes), the top plate, also covered with teflon coated aluminum foil, was positioned such that the mold filled with the melted sample was sandwiched between the two plates. The platens were then pressed together until a force of approximately 5,000 lbs. was obtained. The pressure was then relieved momentarily to allow the release of any entrapped gases, after which a force of 20,000 lbs. was applied to the mold. After 20 minutes at 200°C and 20,000 lbs. force, the mold was cooled by circulating water through the platens, and when the mold temperature reached approximately 75°C, the pressure was relieved and the molded sample removed.

The rheometer test samples were prepared by cutting the molded composite samples to the appropriate sizes by using a band saw. These test samples were also vacuum dried at 80°C before using them in the rheometer.

Data Collection

The rheological data were obtained by using a Rheometrics RMS-800 mechanical spectrometer operated in both steady shear and dynamic oscillatory modes. The RMS-800 can be operated with a controlled sample environment and over a temperature range of -150 to +350°C. Detailed diagrams of the test station and the environmental chamber can be found in the operating manual. Two sets of disks were used during this investigation, and the respective radii were 12.5 and 25 mm. In order

to prevent oxidative degradation, liquid nitrogen was boiled in the system dewar to provide a gaseous nitrogen atmosphere in the sample chamber.

The general operation of the rheometer involved the motion (steady or oscillatory) of the lower disk fixture through a servo motor. The rotational rate and the position of the motor shaft, and subsequently the lower disk, were measured by a tachometer and a rotational variable differential capacitor (RCVD). The command motion of the lower disk was transmitted through the sample to the upper disk which was connected to a force rebalance transducer (FRT). The torque required to maintain the position of the transducer shaft, and thus the upper disk, and the normal force required to maintain a constant disk separation were determined.

Sample temperature in the RMS-800 was maintained through the use of the gas convection oven with PID control. Heat was supplied via an electric gun heater inserted into the environmental chamber. The oven temperature was measured with a type J thermocouple located in the chamber, and a PRT sensor, also located in the environmental chamber, provided the temperature monitoring required for control. Additionally, the lower tool temperature was measured by using a type J thermocouple located on the lower surface of the tool, and it was this temperature that was used to determine when the sample thermal equilibrium was attained.

The precut, dried test samples were individually placed on the lower plate of the instrument, and the upper plate and test station were lowered until contact with the sample occurred. The oven halves were then closed, and the sample and tooling were heated to the desired set

point temperature. When thermal equilibrium was achieved, the top plate was lowered further until the desired gap between the plates was obtained. At that time, the oven was opened, and the excess sample that was squeezed from the gap was removed. The oven was then resealed, and reheating was initiated. When the desired tool temperature reached steady state (no change in tool temperature over a 3-4 minute period), the particular rheological test was initiated.

Auxilliary Procedures

Ashing procedure. The concentrations of the various composite samples were experimentally determined by ashing the samples. Predried sample pellets were loaded into dried, tared, ceramic ashing boats, and the total weight was measured and recorded. The filled boats were then placed in a Fisher Scientific model 184A muffle furnace at 460°C for at least 2 hours. The remaining ash and weigh boat were weighed, and the mass fraction of the filler was determined from the inorganic ash that remained. Component densities were used to convert the inorganic fraction to a volumetric basis, and the calculations accounted for the water hydrated to the CaCO_3 filler.

Ashing experiments were also employed to test possible filler particle migration in the rheometer test sample during the loading process. Samples of the extrudate squeezed from the gap between the disks were ashed as previously outlined, and the remaining test disk was also ashed after completion of the rheological testing.

Intrinsic viscosity measurements. The polymer intrinsic viscosities of several of the composite samples were determined to insure that the preparation and processing of the samples had not resulted in any

significant polymer degradation. Predried composite samples were dissolved in a 50/50 methylethylketone/acetone solution. The resulting solution was then centrifuged for 15-20 minutes at room temperature to remove any CaCO_3 present in the PS composite. The supernatant polymer solution was separated from the CaCO_3 precipitate by decanting the liquid into filtered methanol. The polymer precipitate was then filtered under suction and washed with methanol. Finally, the polymer was dried in a vacuum oven at 50°C until no solvent residue remained, and the dry PS was then redissolved in filtered toluene at various concentrations. The viscosities of these solutions were then measured using Canon-Fenske type capillary viscometers, and the intrinsic viscosities were determined by extrapolating to zero polymer concentration as outlined by Hiemenz (65).

Scanning electron microscopic analyses. Scanning electron microscopy (SEM) was used to determine the degree of dispersion for several selected composite samples. The predried samples were submitted to the Materials Analytical Instrumentation Center at the University of Florida and were freeze fractured and then gold coated under high vacuum. The samples were then observed with a JEOL model JSM-35CF SEM and representative micrographs were obtained.

Modelling work. The model derived by Adams (64) was used to fit the complex viscosity-frequency data obtained from both group 1 and group 2 experiments at 210°C . Since the model has utility in predicting similarly shaped functions, the reduced storage modulus-frequency data at 210°C was used to further test the model. Detailed derivations of the models used appear in (64). In both cases, the slope in the fully developed power-law region was known and so a standard simplex routine,

obtained from Clarkson University, was modified for use with a personal computer and used to determine the remaining model parameters. A copy of the programs used is on file and can be obtained from Dr. Arthur Fricke, University of Florida. The model was not applied to higher temperature data since many of the flow curves at both 235 and 260°C failed to reach the fully developed power-law region. Both models require that either the power-law slope or the distribution standard deviation be determined independently. It is possible to determine a standard deviation by trial and error methods, however this approach was considered to be more of a curve fitting technique than having at least one known parameter value.

RESULTS

The rheological properties of PS composites containing from 2.5 to 30 volume % of both CaCO_3 and rubber fillers were determined over a temperature range of 210-260°C. Both unimodal and bimodal distributions of particle sizes ranging from 0.8 to 20 microns were employed, and the rheological properties were determined over a frequency range of 0.1 to 100 rad/S. The amount of raw data obtained in this investigation was considered to be too extensive to include in this dissertation, however all of the data obtained may be obtained by contacting the Department of Chemical Engineering at the University of Florida.

A recently developed stochastic model developed by Adams (64) to describe the shear rate, molecular weight, and temperature dependence of polymer melt viscosity was used to describe the frequency dependence of both the complex viscosity and the reduced loss modulus (G''/ω^2) of the various PS composites. Finally, the results of the study were analyzed and semi-quantitatively described using concepts and a model (47) derived from percolation theory.

Figures 5 through 10 display the frequency dependence of Groups 1, 2, and 3 composites at 210°C along with the Adams model predictions, and Figures 11 through 14 show both the data and the model predictions of the reduced storage moduli of Groups 1 and 2 materials as functions of frequency also at 210°C. The effect of frequency on the reduced storage modulus for the Group 3 samples are given in Figures 15 and 16, and

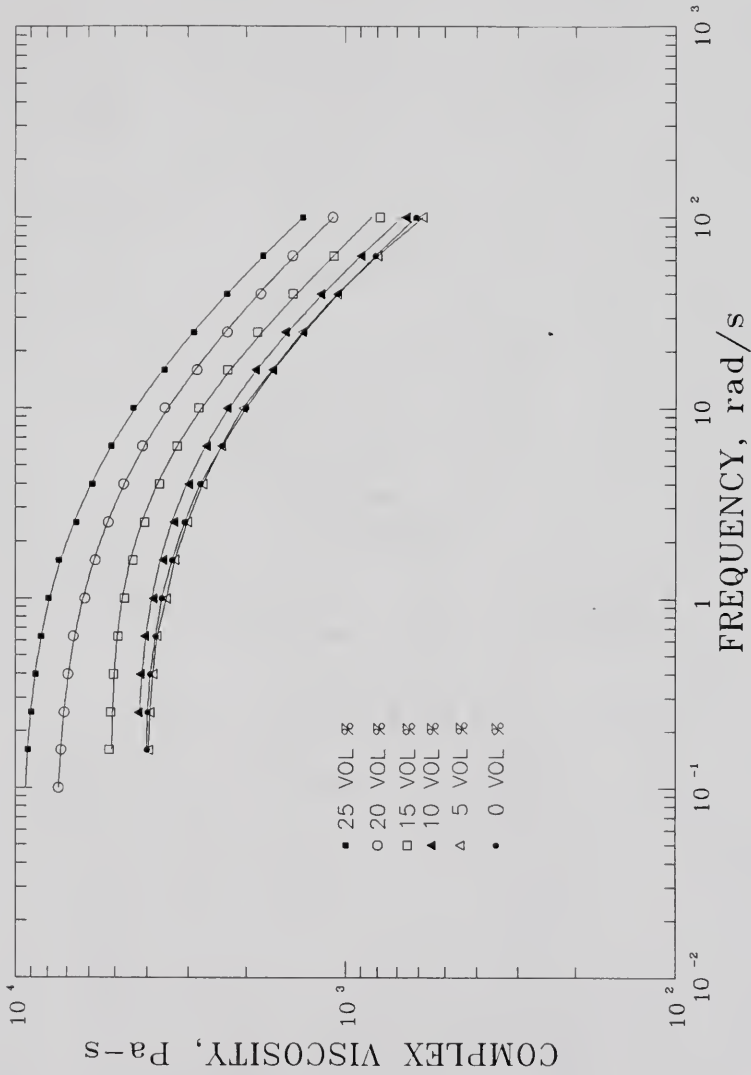


Figure 5. The Effect of Nominal Concentration of 20 Micron CaCO_3 on the Complex Viscosity of Polystyrene Composites at 210°C . Included are the Adams Model Predictions (—).

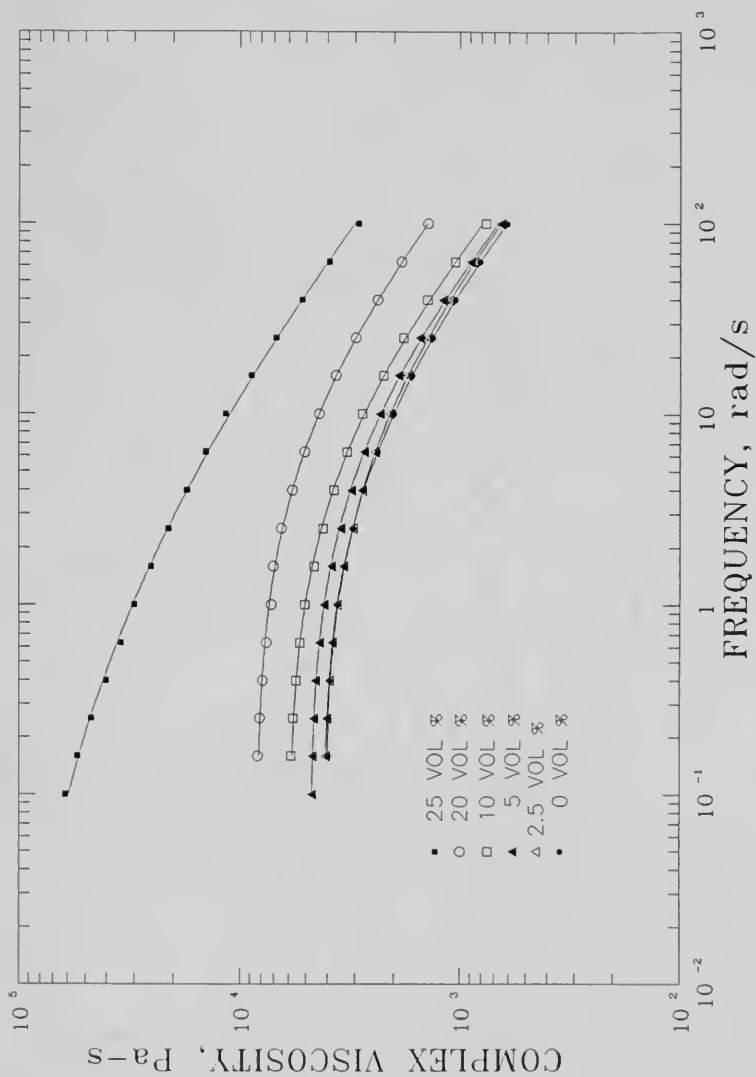


Figure 6. The Effect of Nominal Concentration of 2 Micron CaCO_3 on the Complex Viscosity of Polystyrene Composites at 210°C . Included are the Adams Model Predictions (—).

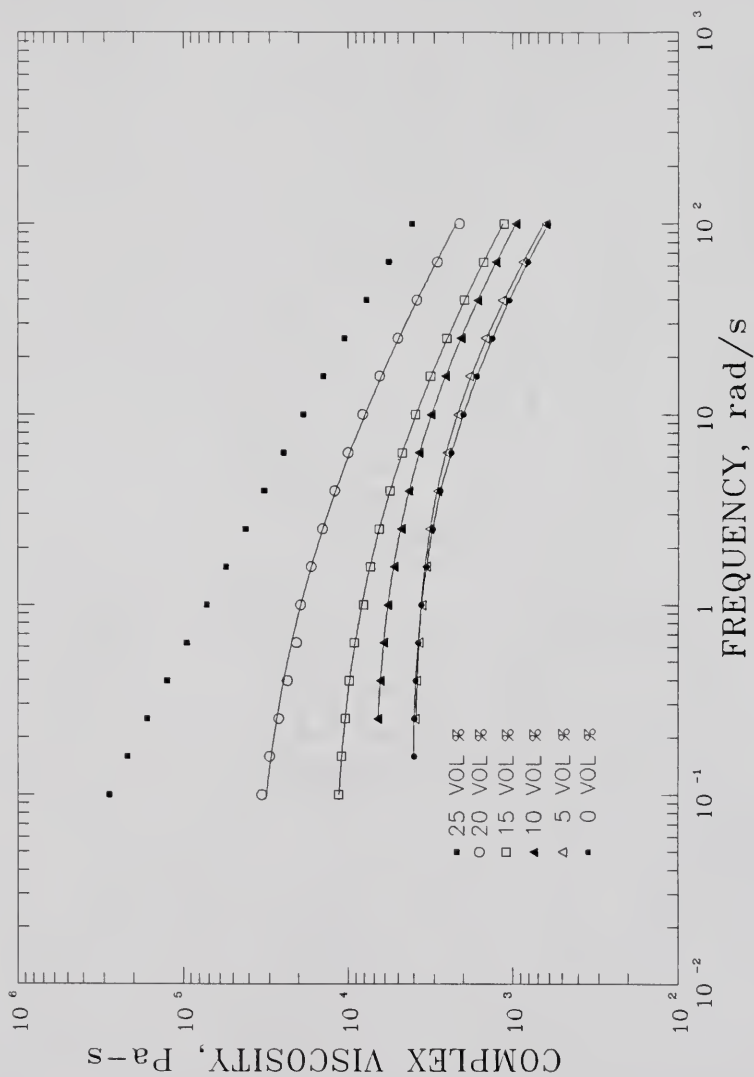


Figure 7. The Effect of Nominal Concentration of 0.8 Micron CaCO_3 on the Complex Viscosity of Polystyrene Composites at 210°C . Included are the Adams Model Predictions (—).

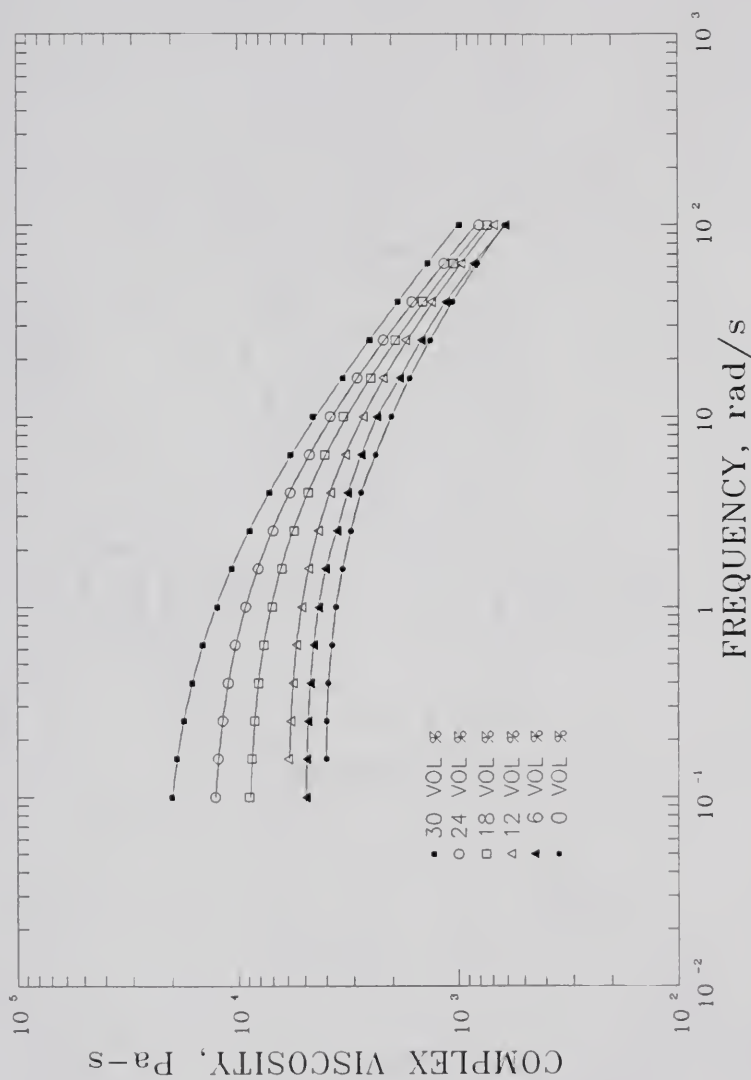


Figure 8. The Effect of Nominal Concentration of 1.9 Micron Rubber on the Complex Viscosity of Polystyrene Composites at 210°C. Included are the Adams Model Predictions (—).

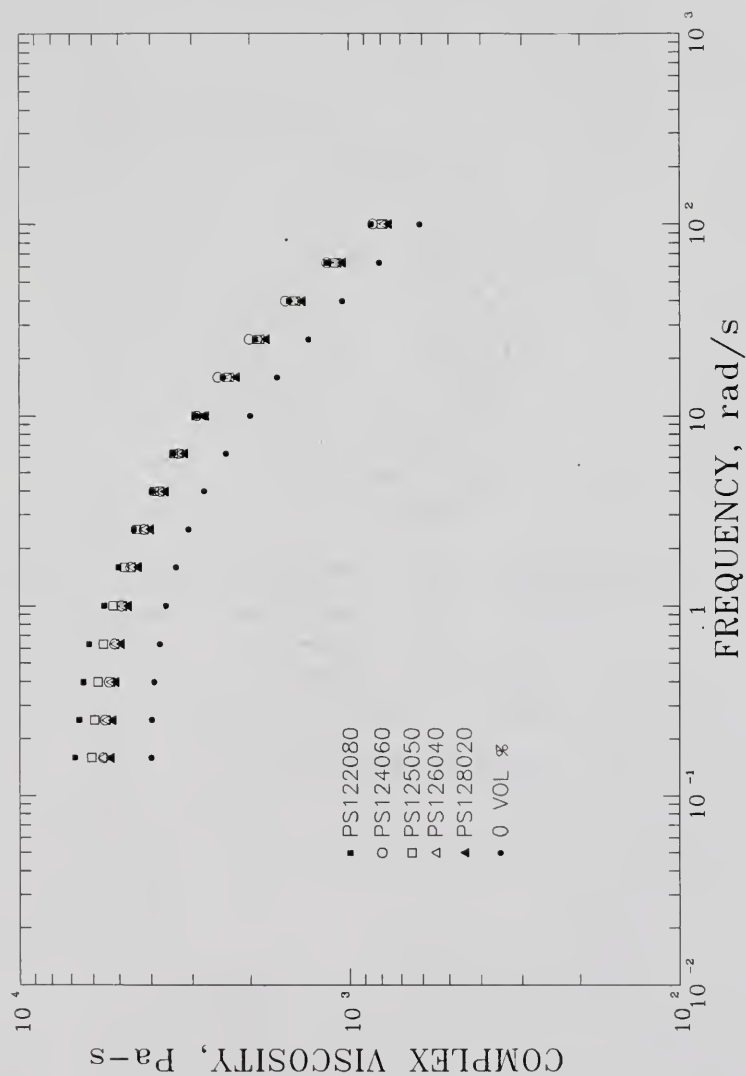


Figure 9. The Effect of CaCO_3 Particle Size Distribution on the Complex Viscosity of Polystyrene Composites at 210°C . Nominal Concentrations are 12 vol. %.

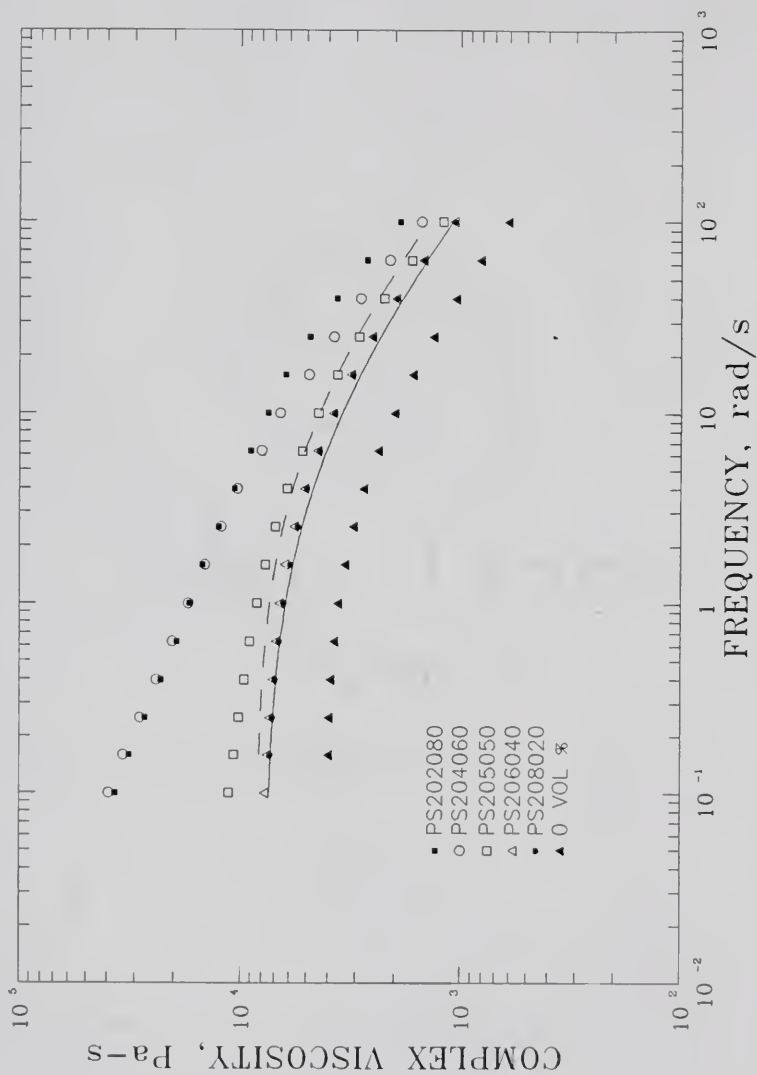


Figure 10. The Effect of CaCO_3 Particle Size Distribution on the Complex Viscosity of Polystyrene Composites at 210°C . Nominal Concentrations are 20 vol. %. Included are the Adams Model Predictions for PS2020 (—) and PS202 (---).

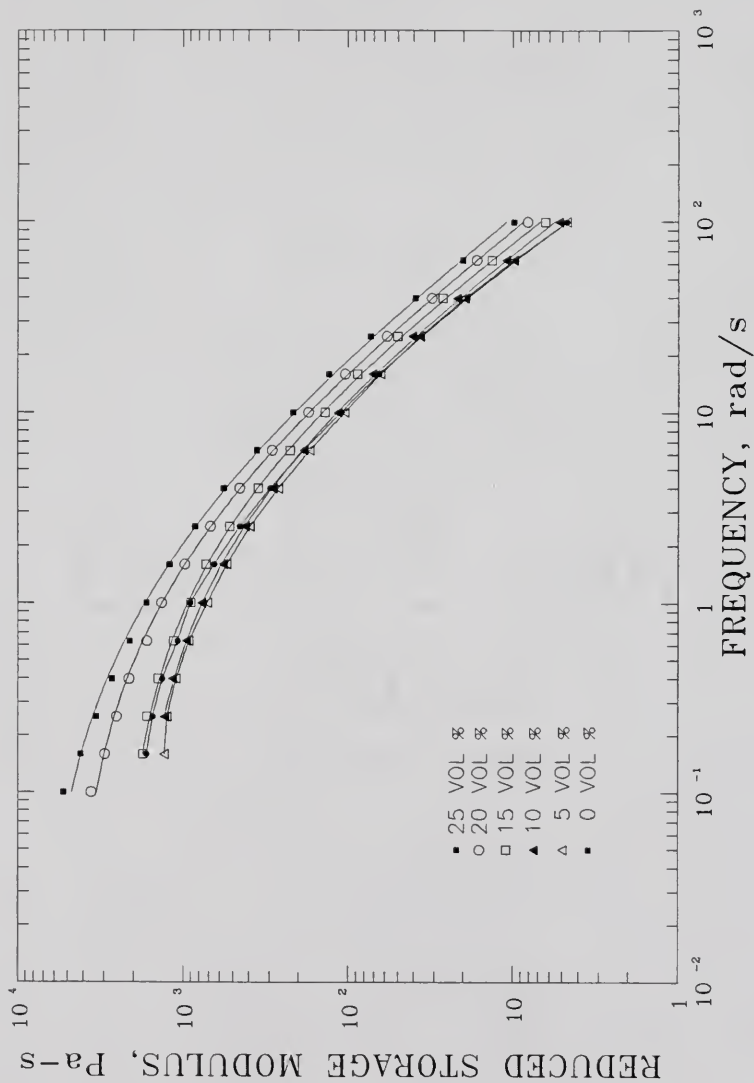


Figure 11. The Effect of Nominal Concentration of 20 Micron CaCO_3 on the Reduced Storage Modulus (G'/ω^2) of Polystyrene Composites at 210°C . Included are the Adams Model Predictions (—).

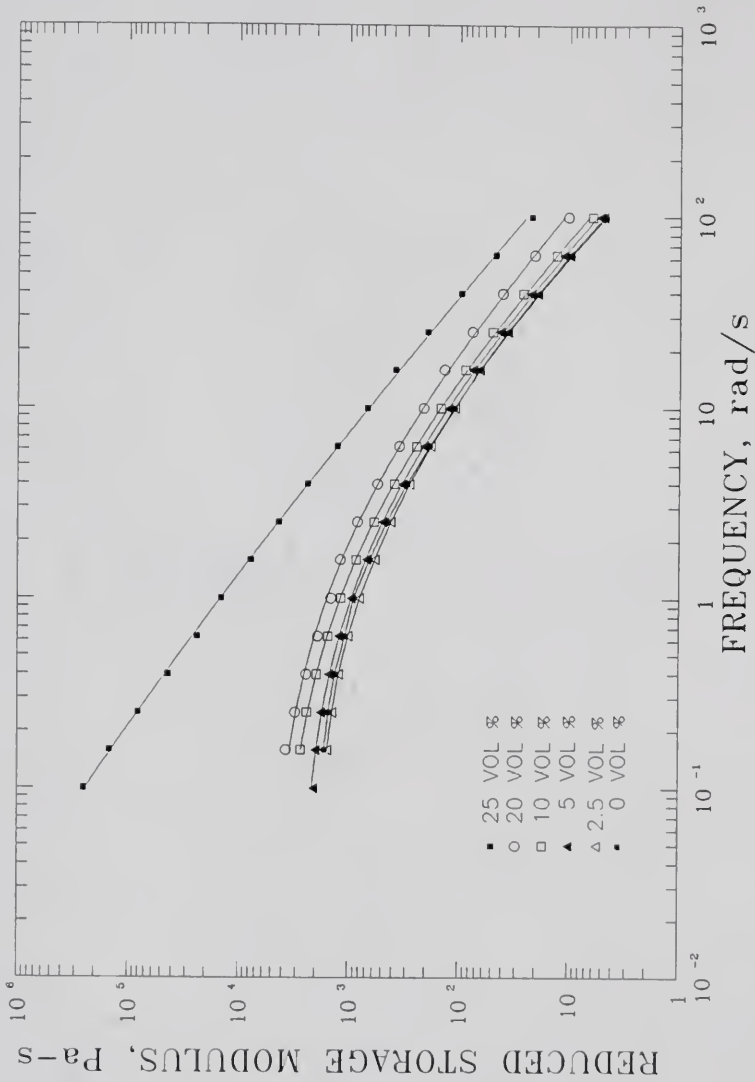


Figure 12. The Effect of Nominal Concentration of 2 Micron CaCO_3 on the Reduced Storage Modulus (G'/ω^2) of Polystyrene Composites at 210°C . Included are the Adams Model Predictions (—).

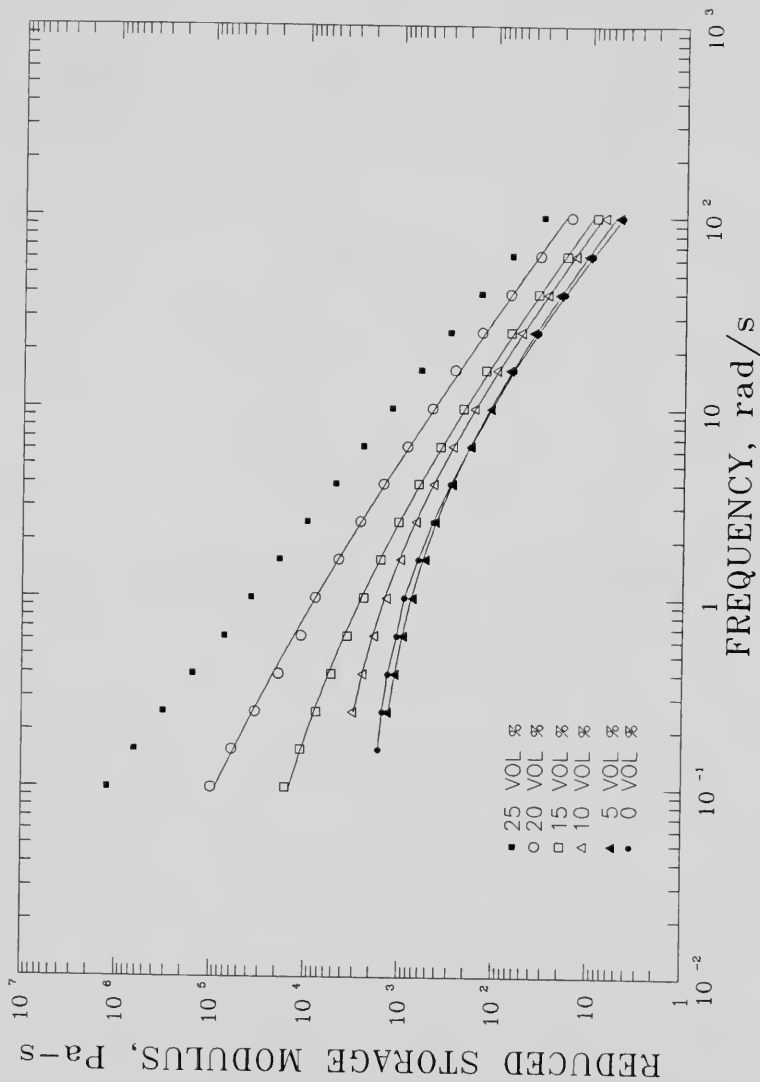


Figure 13. The Effect of Nominal Concentration of 0.8 Micron CaCO_3 on the Reduced Storage Modulus (G'/ω^2) of Polystyrene Composites at 210°C . Included are the Adams Model Predictions (—).

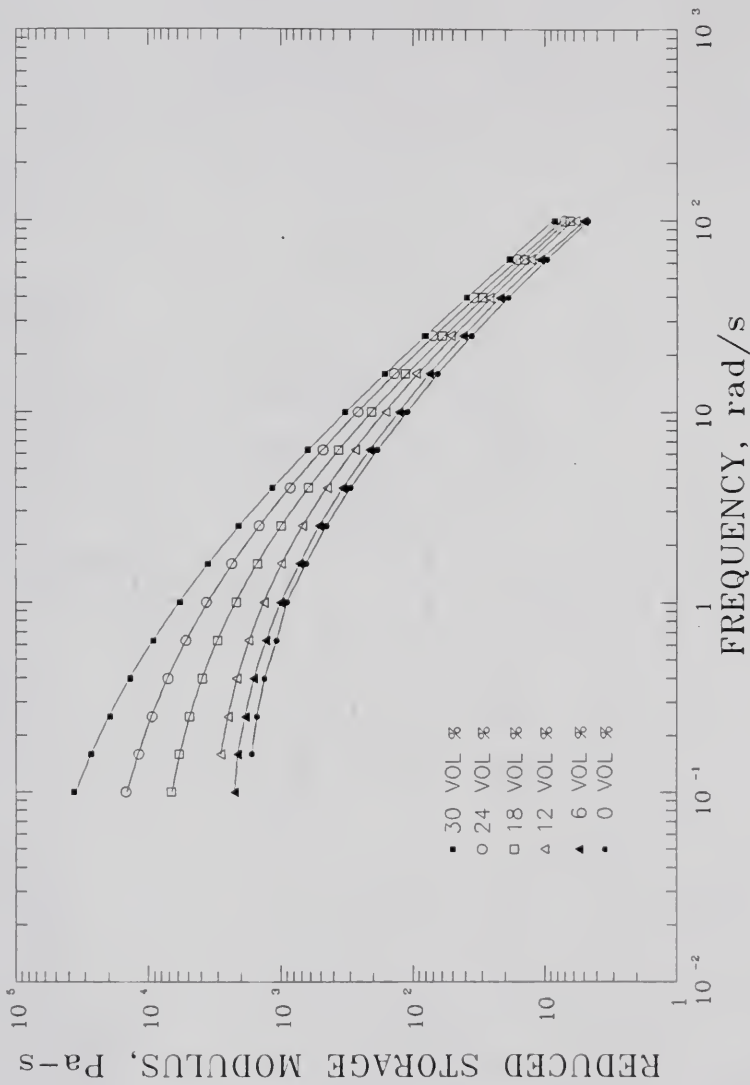


Figure 14. The Effect of Nominal Concentration of 1.9 Micron Rubber on the Reduced Storage Modulus (G'/ω^2) of Polystyrene Composites at 210°C. Included are the Adams Model Predictions (—).

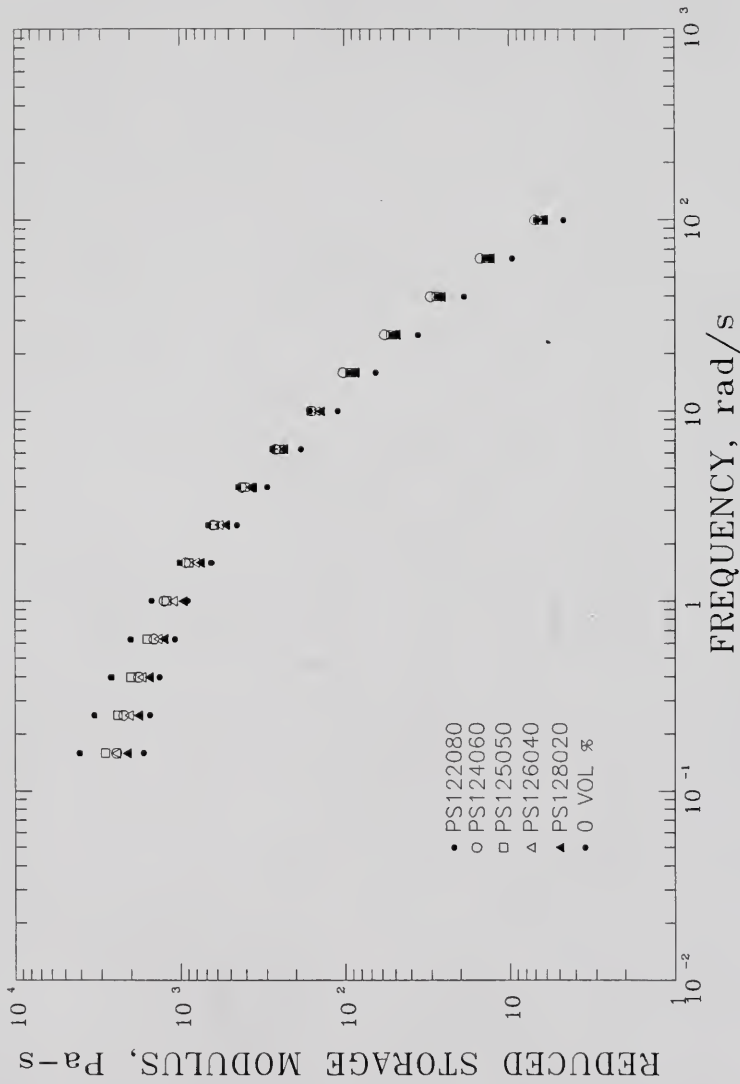


Figure 15. The Effect of CaCO_3 Particle Size Distribution on the Reduced Storage Modulus (G'/ω^2) of Polystyrene Composites at 210°C . Nominal Concentrations are 12 vol. %.

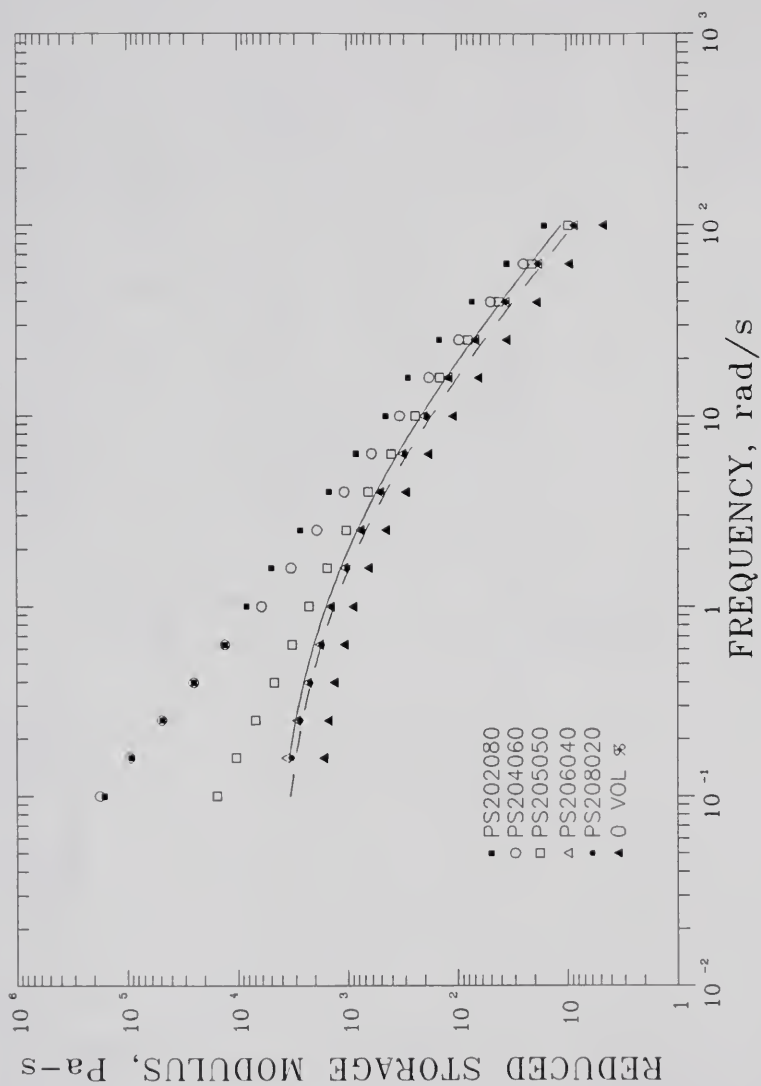


Figure 16. The Effect of CaCO_3 Particle Size Distribution on the Reduced Storage Modulus (G'/ω^2) of Polystyrene Composites at 210°C . Nominal Concentrations are 20 vol. %. Included are the Adams Model Predictions for PS2020 (---) and PS202 (—).

similarly, the frequency dependence of the reduced loss modulus for all three groups of materials are contained in Figures 17 through 22.

The flow curves depicting the effects of particle size and type of filler at 210°C and at filler concentrations both above and below the theoretical critical percolation concentration are shown in Figures 23 and 24. The effect of filler concentration on the limiting frequency reduced complex viscosity of both CaCO_3 and rubber filled PS composites at 210°C appear in Figures 25 through 28. Included in these figures are the Campbell and Forgacs model predictions for both hexagonal and cubic maximum packing geometries. The various modelling parameters determined from the Adams model fit of the complex viscosity-frequency data at 210°C are shown as functions of the filler specific surface area in Figures 29 through 31. A comparison of the Cox-Merz (66) approximation for selected materials appear in Figures 32 and 33. The steady shear viscosities in these figures were determined by using an Instron capillary rheometer (ICR) model 3211. The ICR results were determined in a separate project by Kelly (67).

The typical temperature dependence of the composite flow curves is shown in Figure 34, and the effects of oxidative degradation of the rheological test sample on the rheological measurements for a selected composite and the neat polymer appear in Figures 35 and 36. Finally, the quality of the compounding and the dispersion of various composites was investigated using SEM, and the micrographs appear in Figures 37 through 39.

The actual volume fractions of the various CaCO_3 composites used are given in Tables 5 and 6. These results were obtained by ashing the composite samples as previously described. It should be noted that the

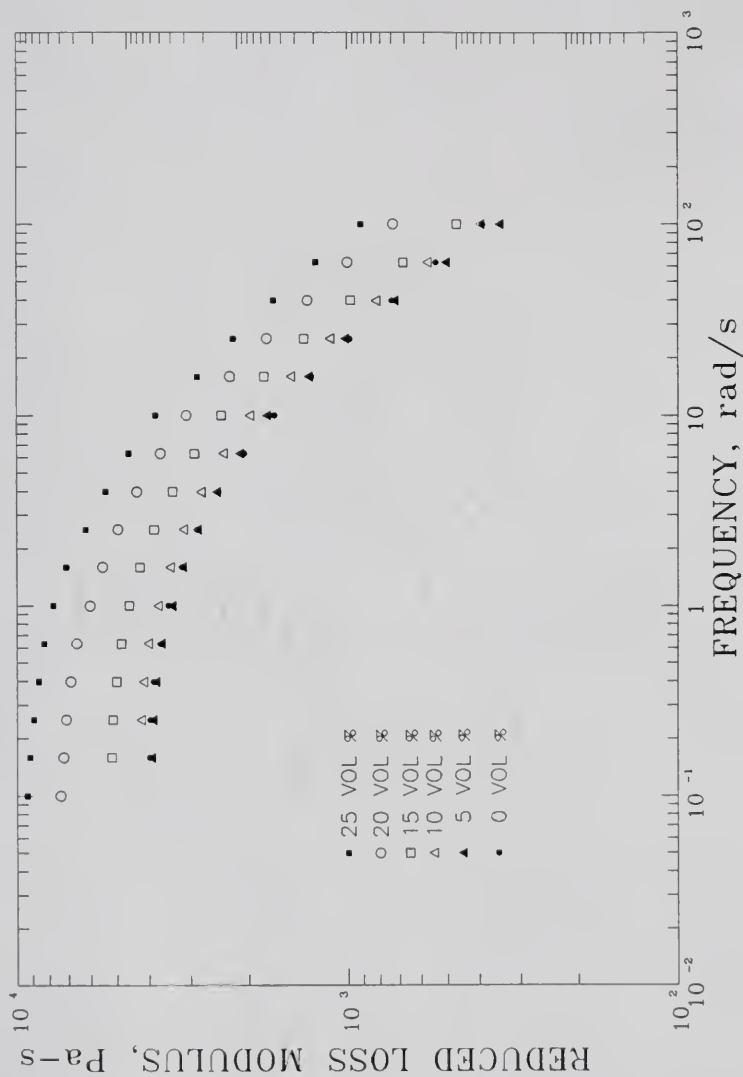


Figure 17. The Effect of Nominal Concentration of 20 Micron CaCO_3 on the Reduced Loss Modulus (G''/ω) of Polystyrene Composites at 210°C .

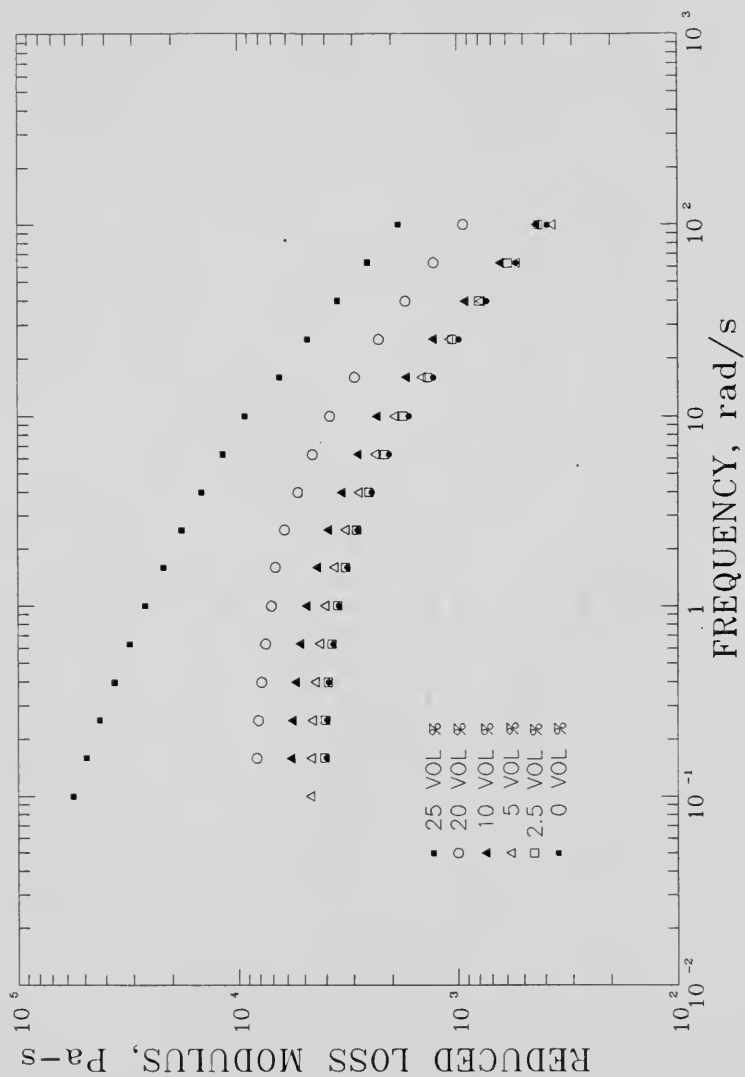


Figure 18. The Effect of Nominal Concentration of 2 Micron CaCO_3 on the Reduced Loss Modulus (G''/ω) of Polystyrene Composites at 210°C .

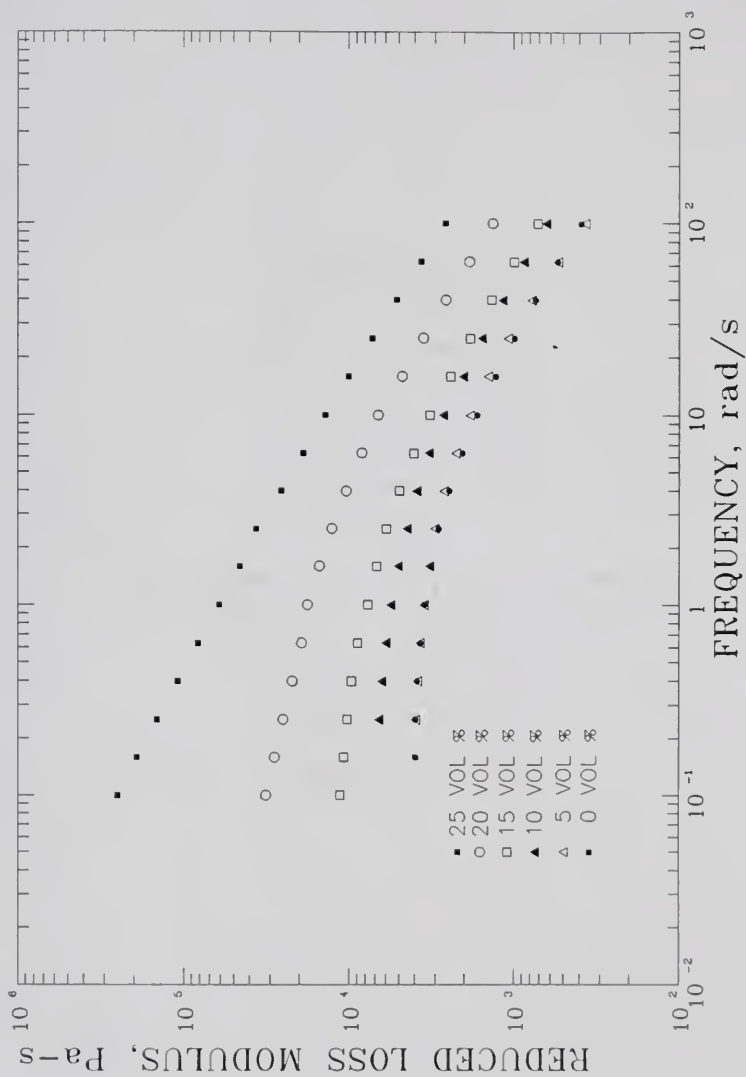


Figure 19. The Effect of Nominal Concentration of 0.8 Micron CaCO_3 on the Reduced Loss Modulus (G''/ω) of Polystyrene Composites at 210°C .

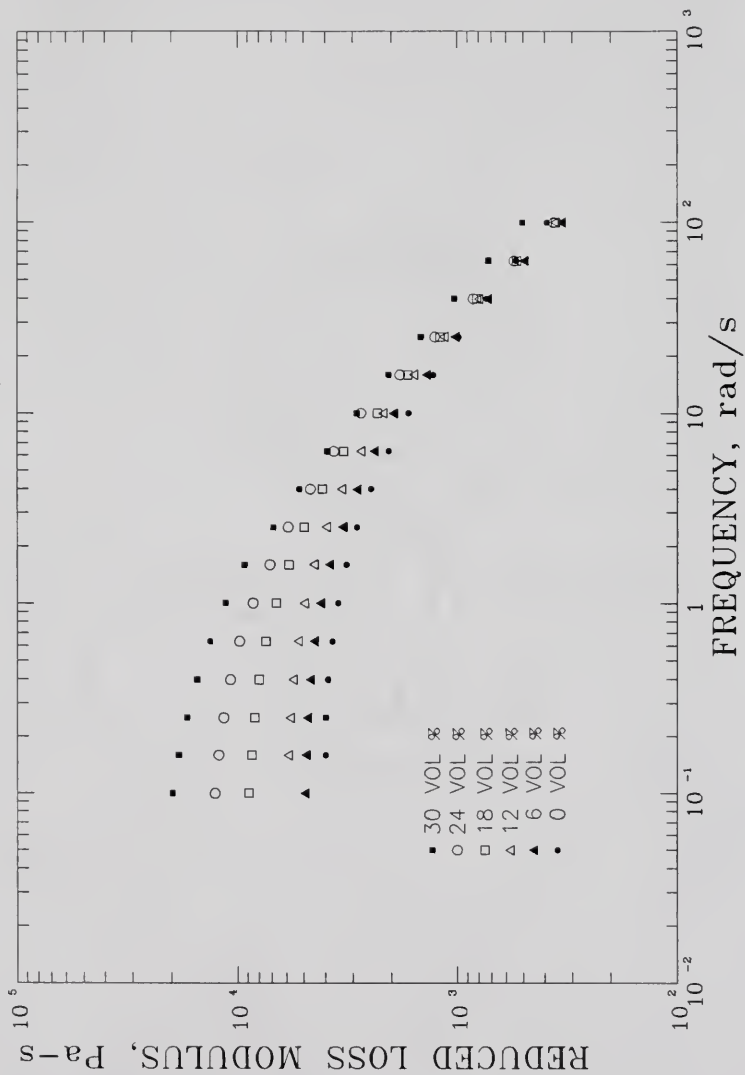


Figure 20. The Effect of Nominal Concentration of 1.9 Micron Rubber on the Reduced Modulus (G''/ω) of Polystyrene Composites at 210°C.

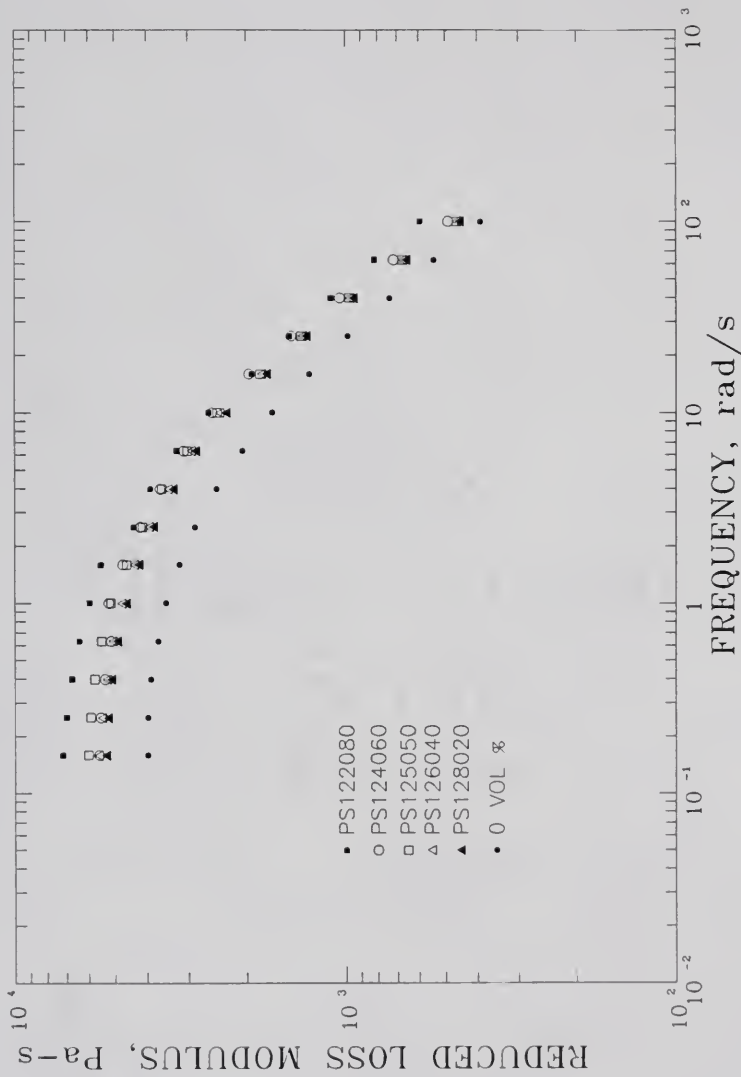


Figure 21. The Effect of CaCO_3 Particle Size Distribution on the Reduced Loss Modulus (G''/ω) of Polystyrene Composites at 210°C . Nominal Concentrations are 12 vol. %.

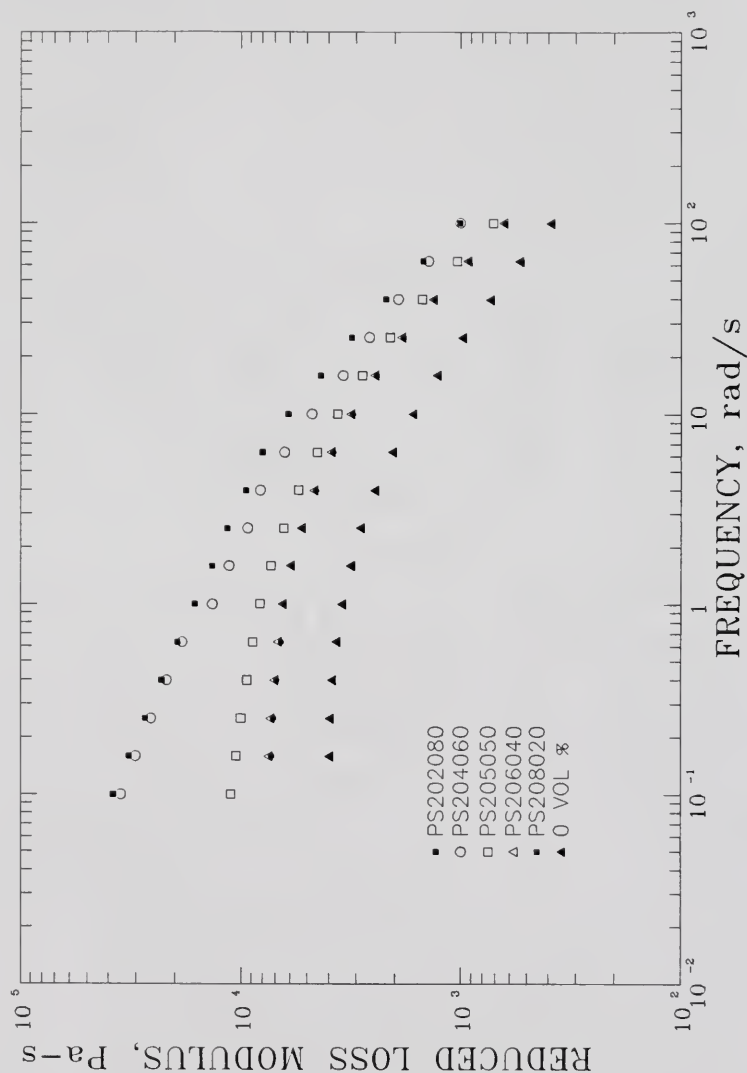


Figure 22. The Effect of CaCO_3 Particle Size Distribution on the Reduced Loss Modulus (G''/ω) of Polystyrene Composites at 210°C . Nominal Concentrations are 20 vol. %.

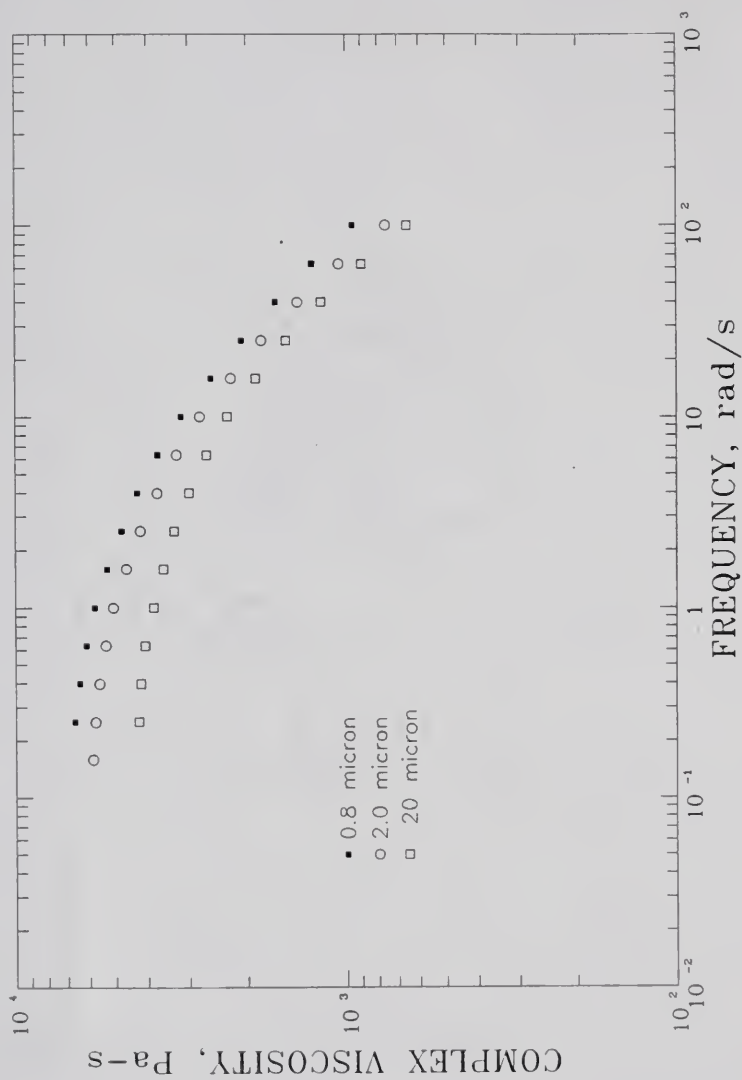


Figure 23. The Effect of CaCO_3 Particle Size on the Complex Viscosity of Polystyrene Composites at 210°C . Nominal Concentrations are 10 vol. %.

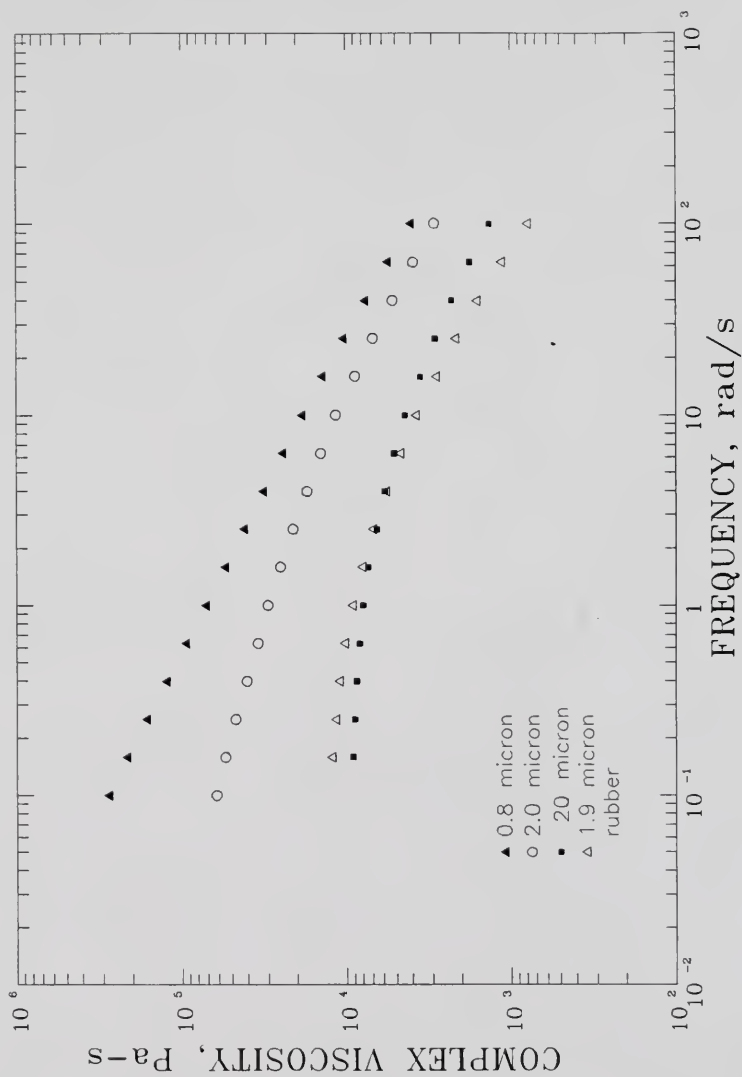


Figure 24. The Effect of Both CaCO_3 and Rubber Particle Size on the Complex Viscosity of Polystyrene Composites at 210°C . Nominal Concentrations are 25 vol. %.

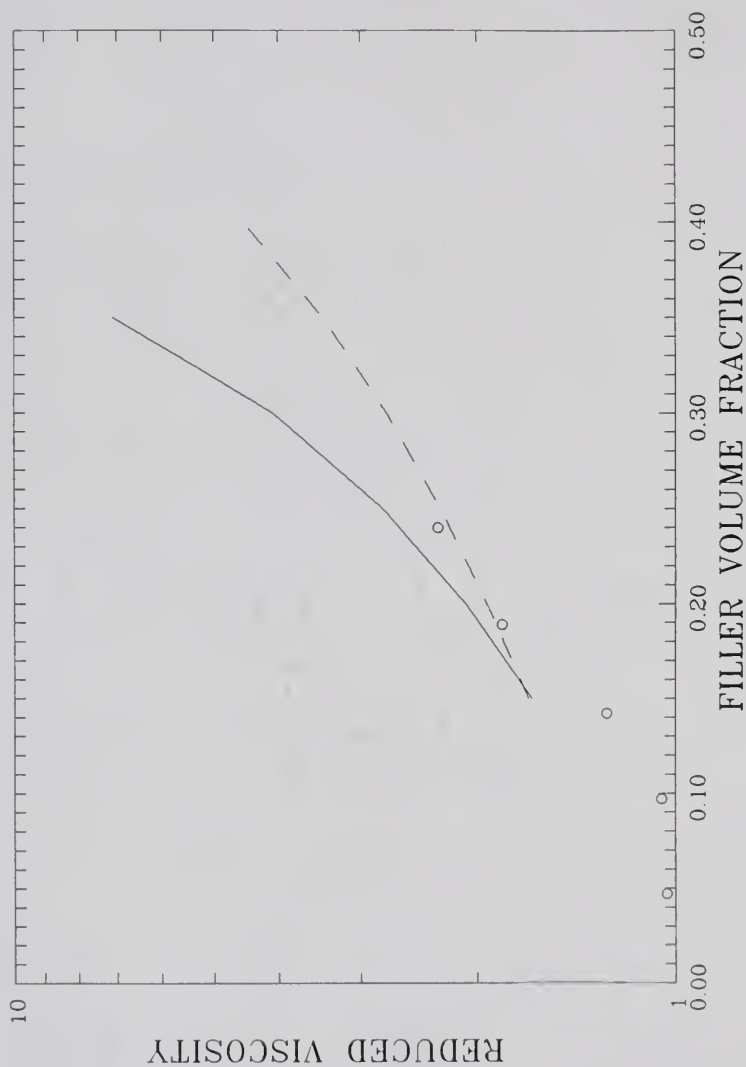


Figure 25. The Effect of Concentration of 20 Micron CaCO_3 on the Reduced Viscosity (at limiting frequency) of Polystyrene Composites at 210°C . Included are the Campbell and Forgacs Model Predictions at $\phi_m = 0.74$ (---) and at $\phi_m = 0.524$ (—).

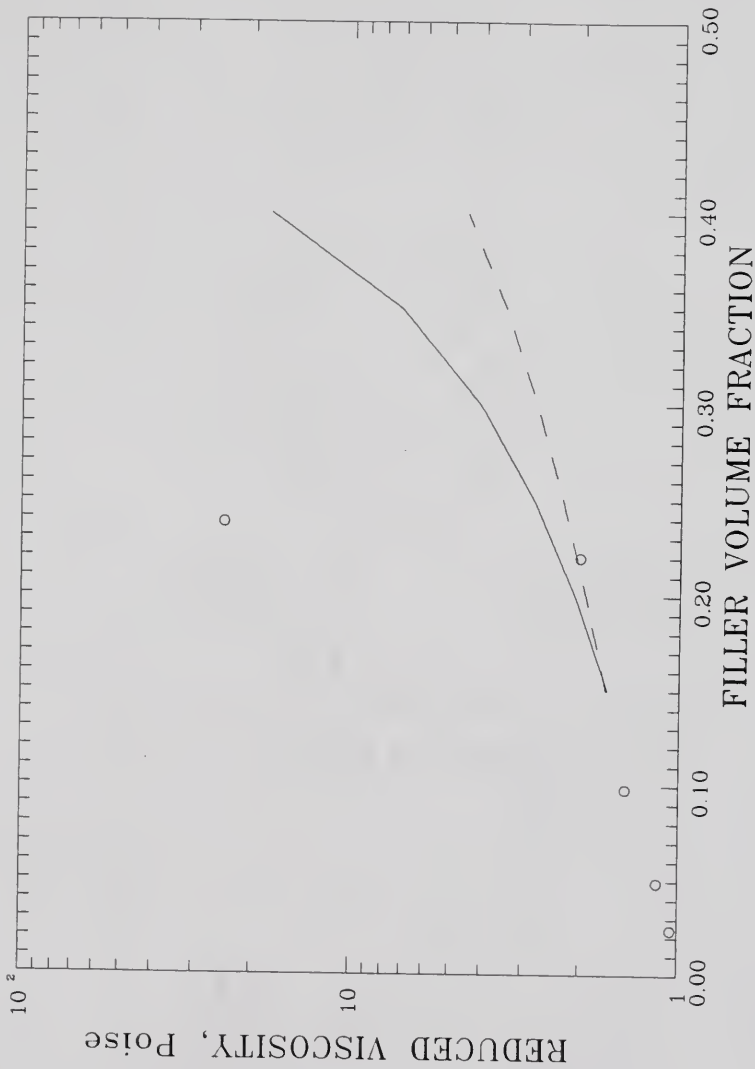


Figure 26. The Effect of Concentration of 2 Micron CaCO_3 on the Reduced Viscosity (at limiting frequency) of Polystyrene Composites at 210°C . Included are the Campbell and Fogacs Model Predictions at $\phi_m = 0.74$ (---) and at $\phi_m = 0.524$ (___).

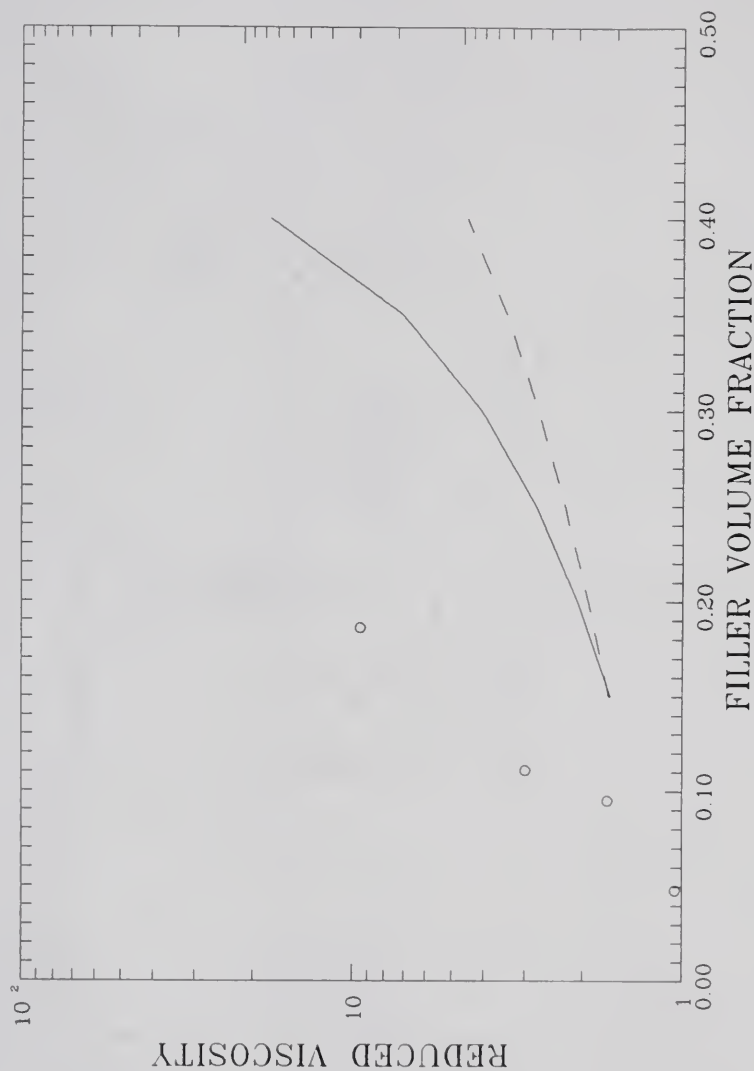


Figure 27. The Effect of Concentration of 0.8 Micron CaCO_3 on the Reduced Viscosity (at limiting frequency) of Polystyrene Composites at 210°C . Included are the Campbell and Forgacs Model Predictions at $\phi_m = 0.74$ (---) and at $\phi_m = 0.524$ (—).

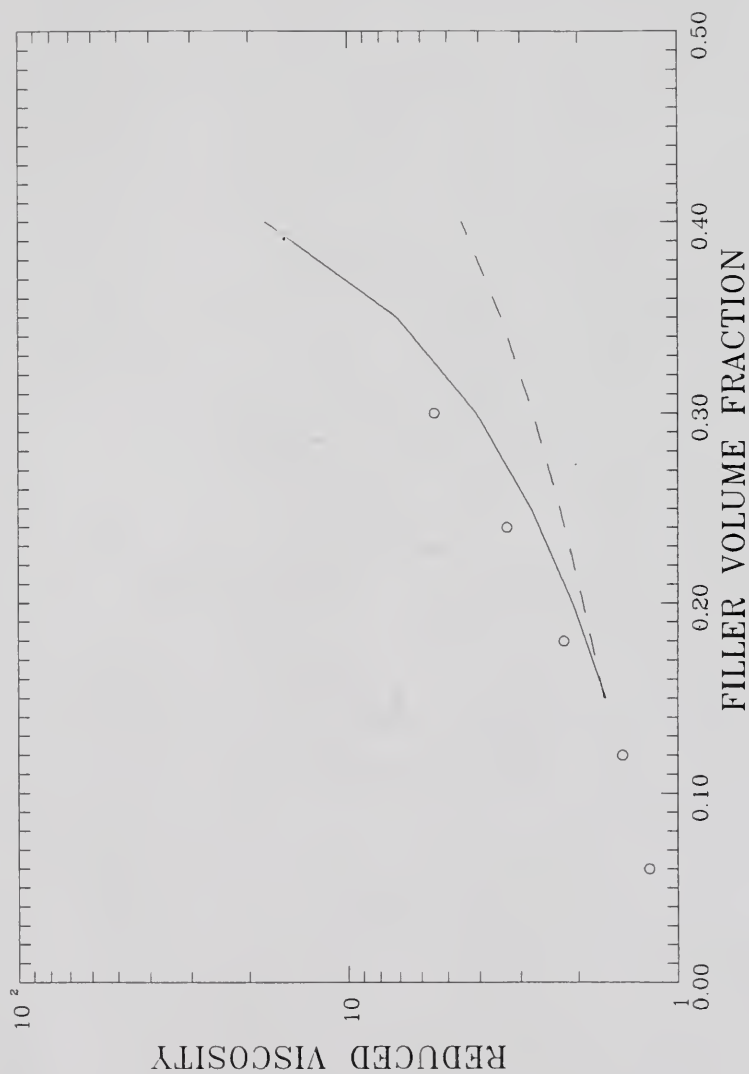


Figure 28. The Effect of Concentration of 1.9 Micron Rubber on the Reduced Viscosity (at limiting frequency) of Polystyrene Composites at 210°C. Included are the Campbell and Forgacs Model Predictions at $\phi_m = 0.74$ (---) and at $\phi_m = 0.524$ (—).

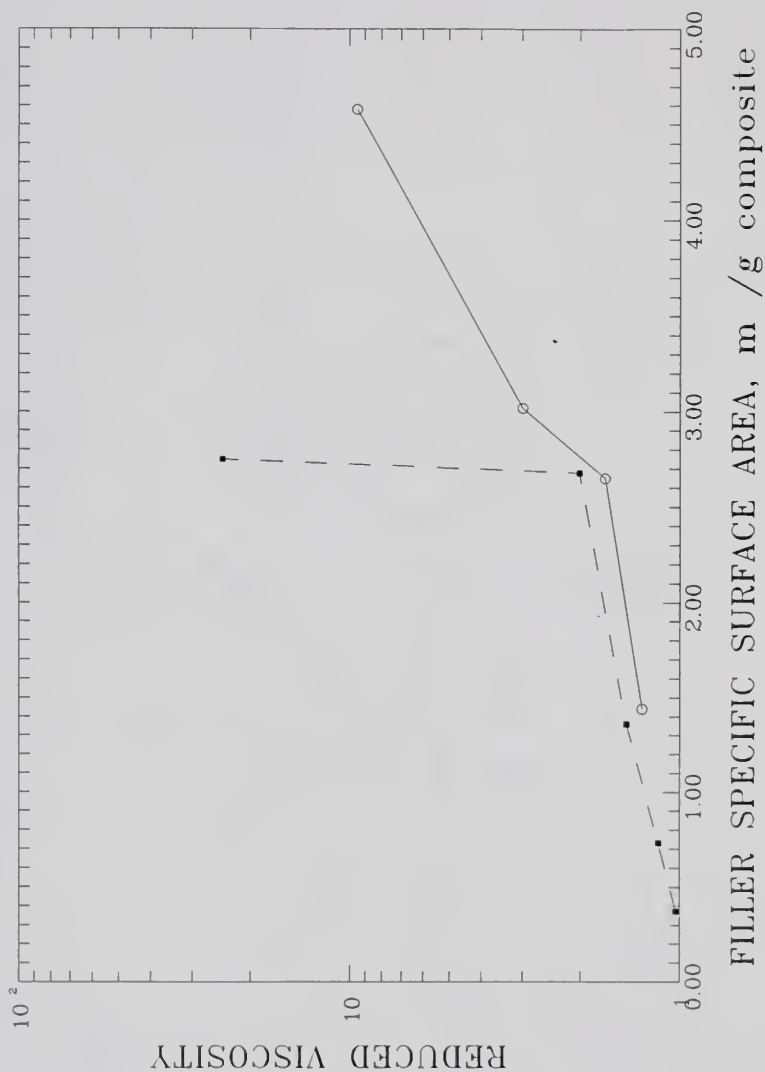


Figure 29. The Effect of Filler Specific Surface Area on the Reduced Viscosity (at limiting frequency as predicted by the Adams Model) of Polystyrene Composites at 210°C. Fillers are 2 Microns CaCO₃ (---) and 0.8 Micron CaCO₃ (—).

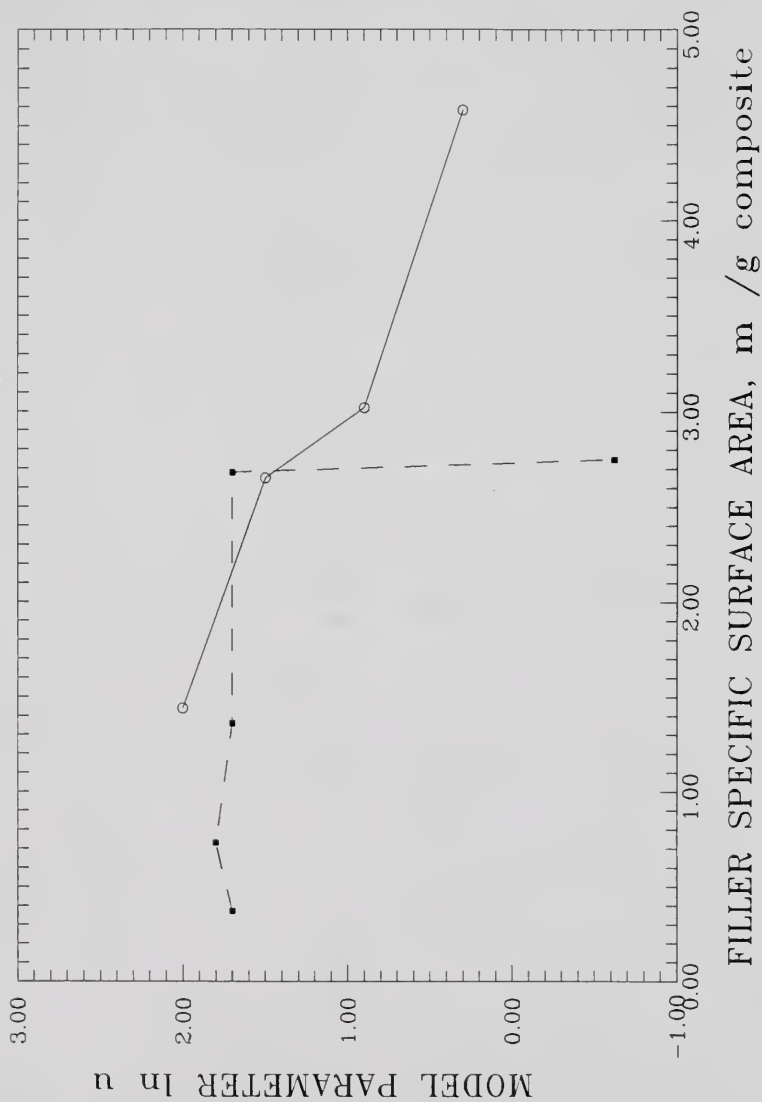


Figure 30. The Effect of Filler Specific Surface Area on the Adams Model Parameter, $\ln u$, for 2 Micron CaCO_3 (---) and 0.8 Micron CaCO_3 (___) Filled Polystyrene Composites at 210°C.

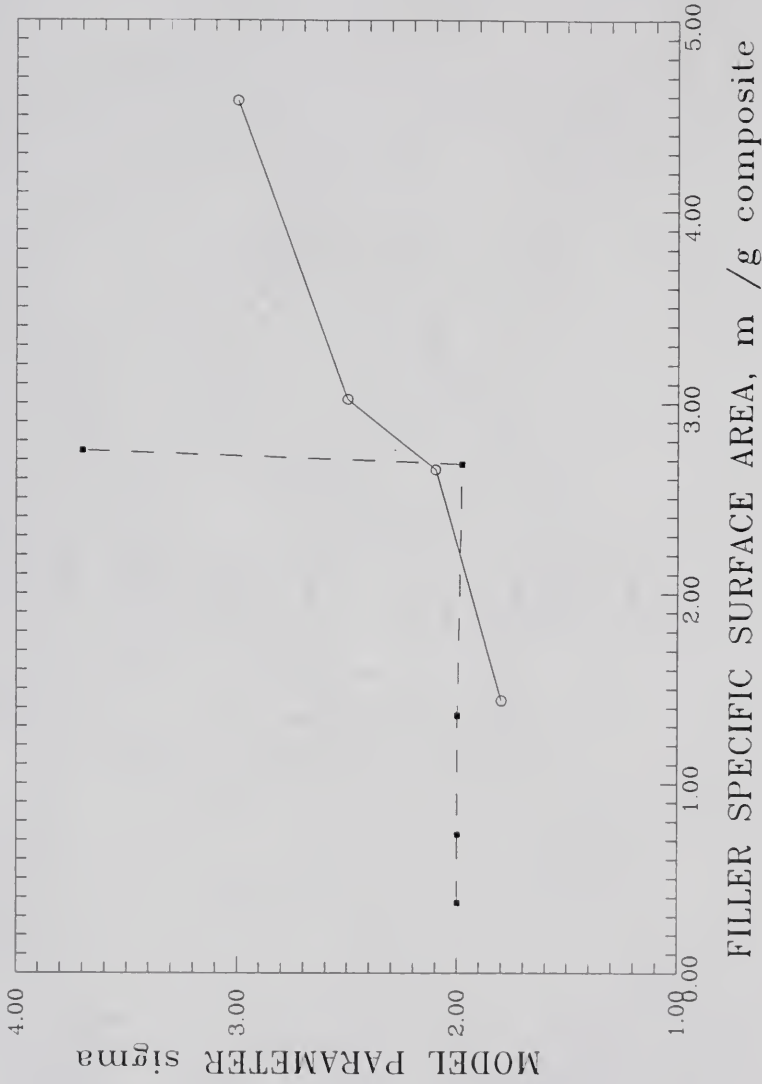


Figure 31. The Effect of Filler Specific Surface Area on the Adams Model Parameter, σ , for 2 Micron CaCO_3 (---) and 0.8 Micron CaCO_3 (___) Filled Polystyrene Composites at 210°C.

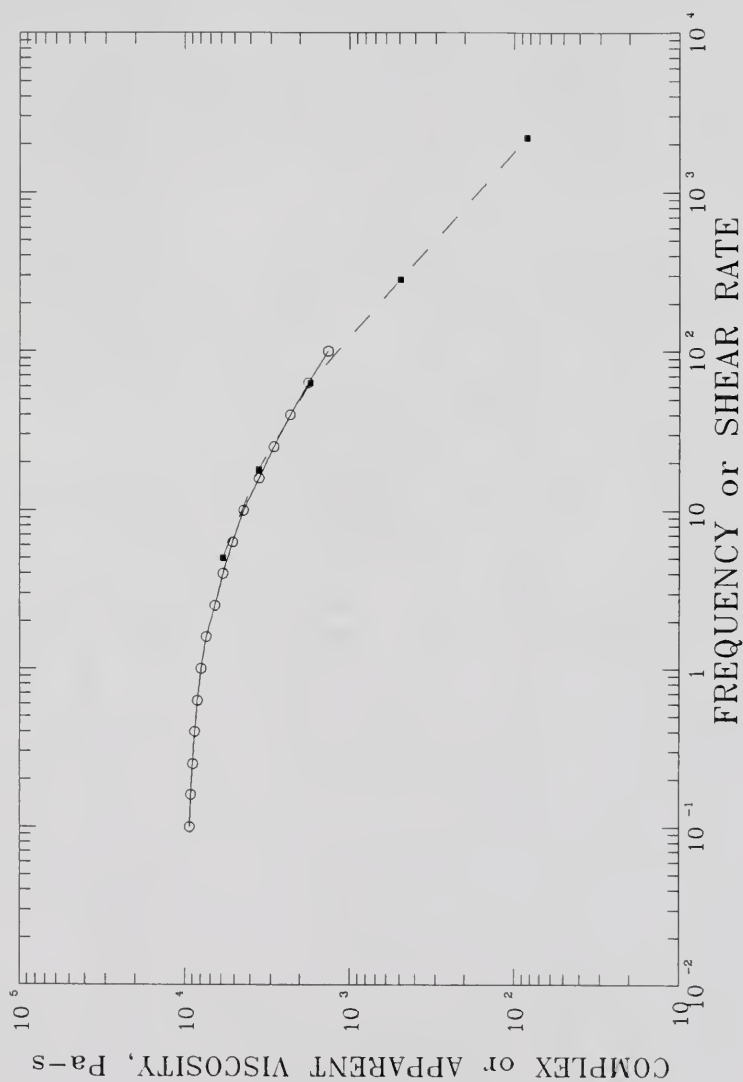


Figure 32. A Comparison of the Cox-Merz Approximation for PS2520 at 210°C.
(Complex Viscosity = —; Apparent Viscosity = ---).

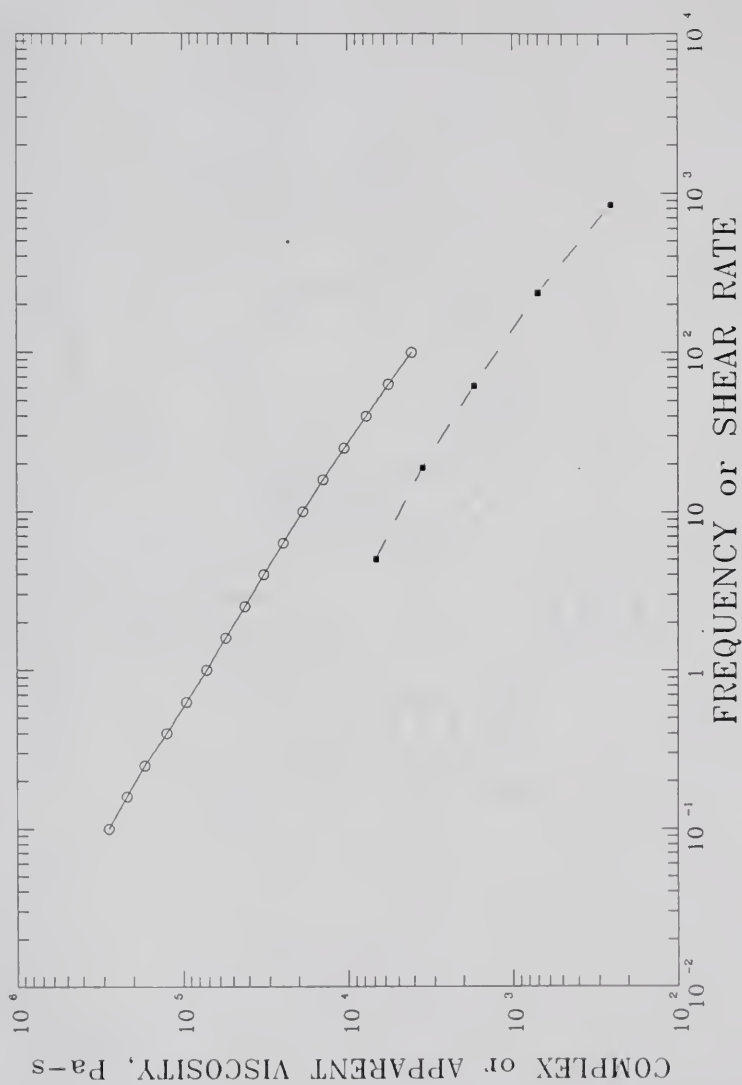


Figure 33. A Comparison of the Cox-Merz Approximation for PS2508 at 210°C. (Complex Viscosity = —; Apparent Viscosity = ---).

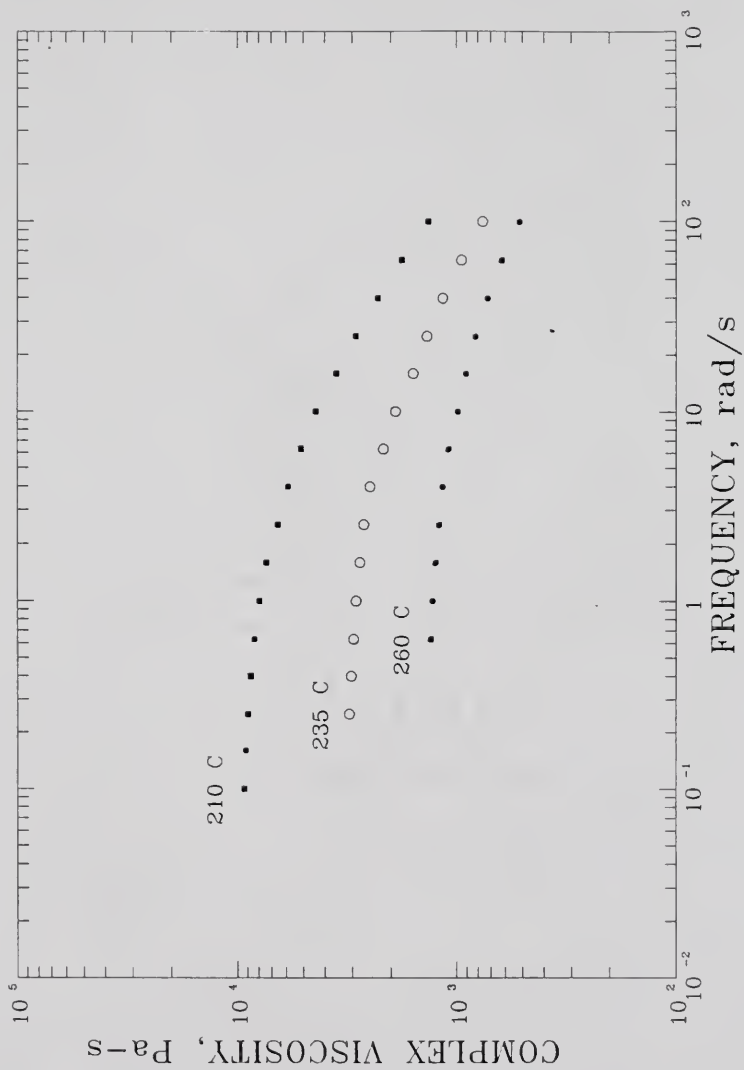


Figure 34. The Temperature Dependence of the Complex Viscosity of PS2520. (Temperature in $^{\circ}\text{C}$).

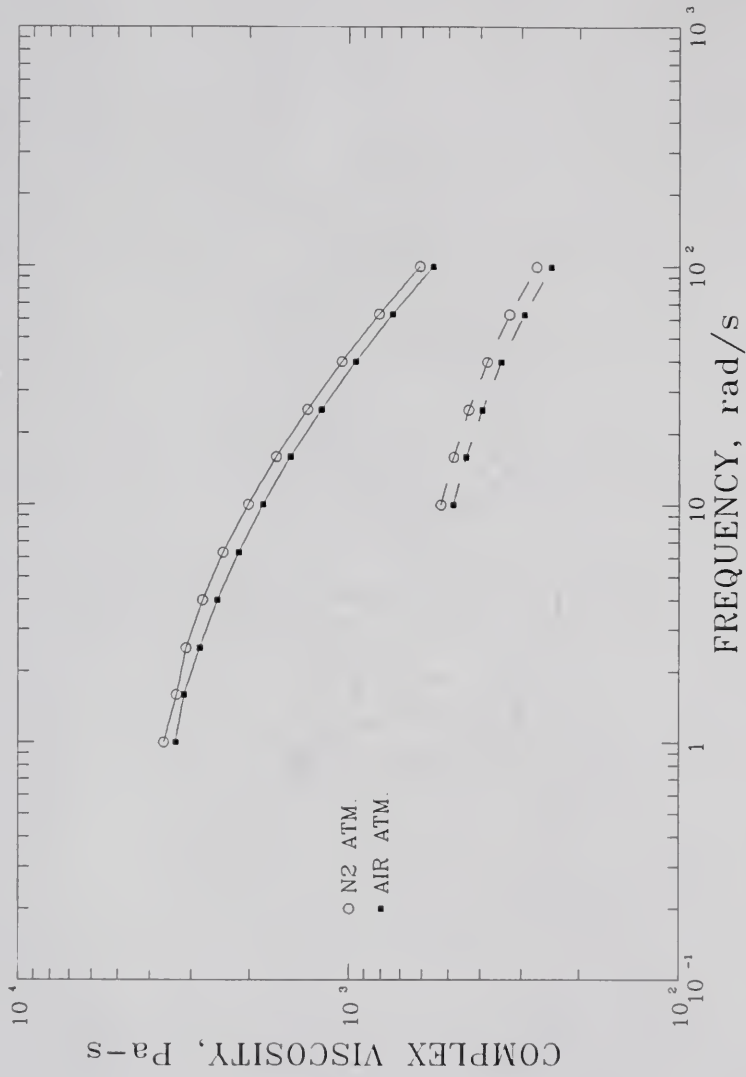


Figure 35. The Effect of Oxidative Degradation on the Complex Viscosity of Polystyrene at 210°C (—) and at 260°C (---).

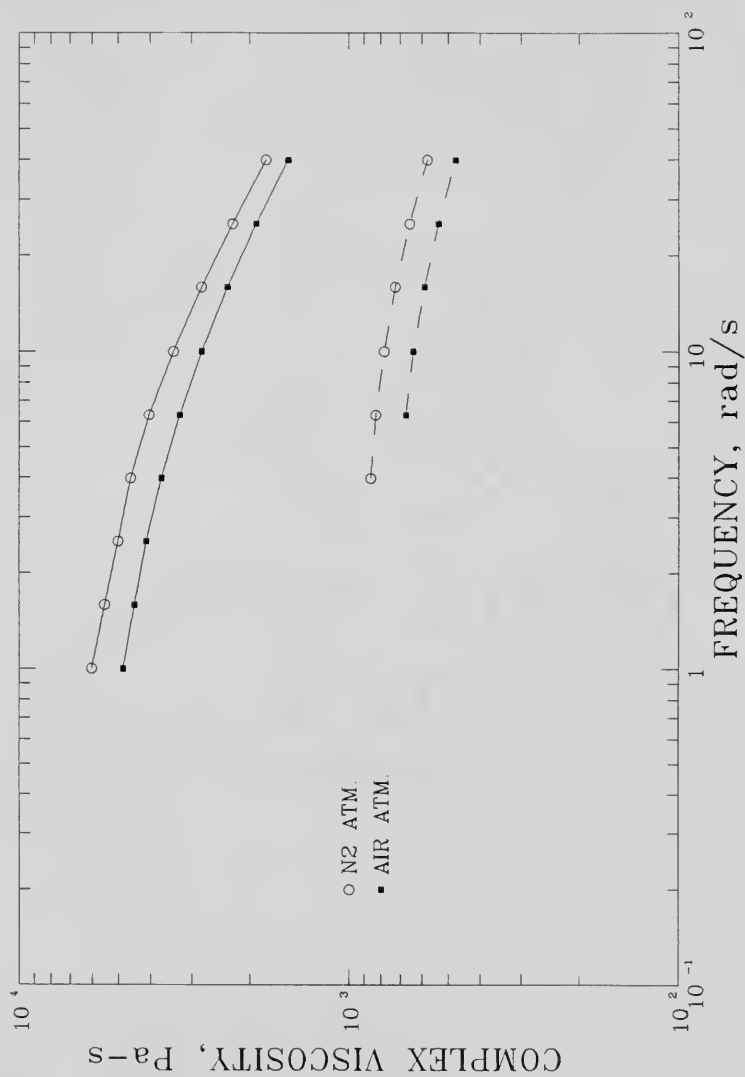


Figure 36. The Effect of Oxidative Degradation on the Complex Viscosity of PS2020 at 210°C (—) and at 260°C (---).

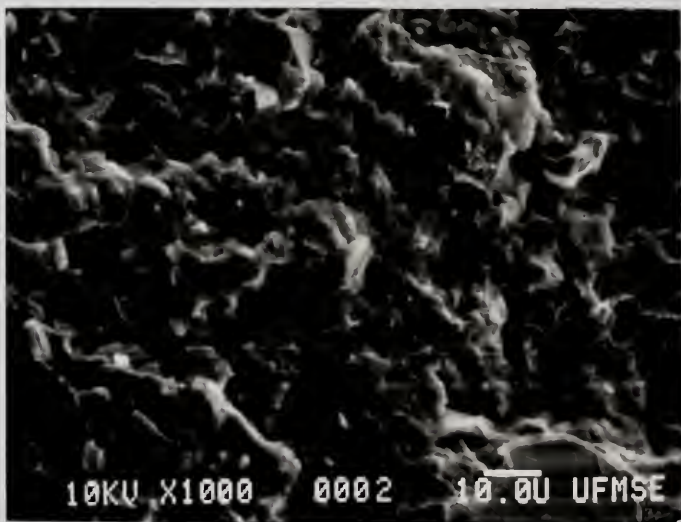
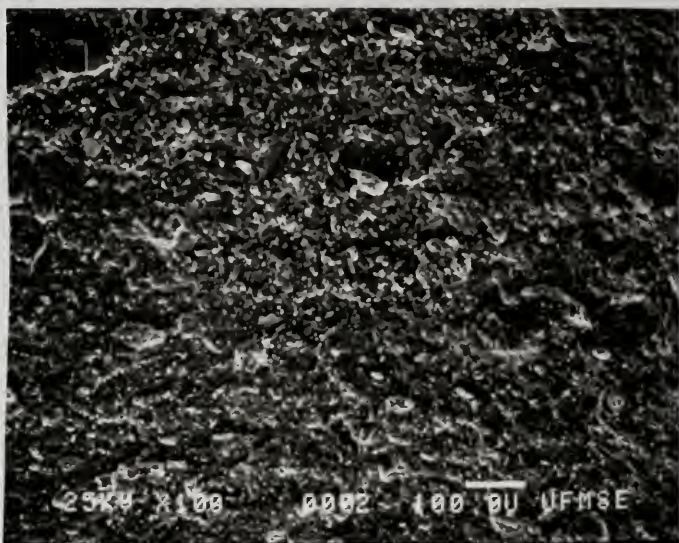


Figure 37. SEM Micrographs of PS2520.

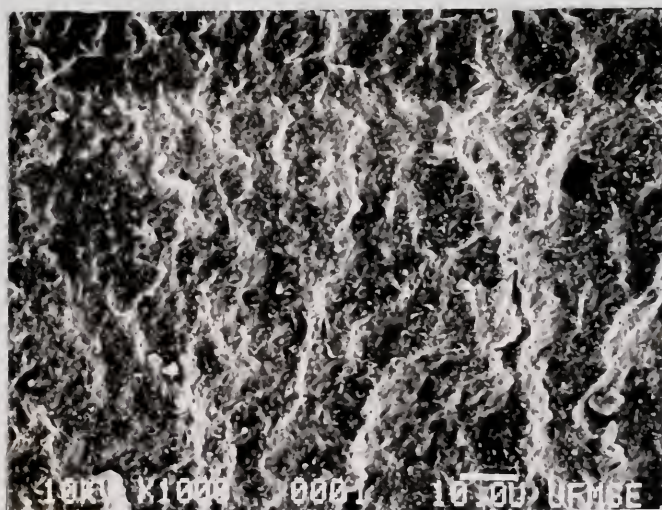
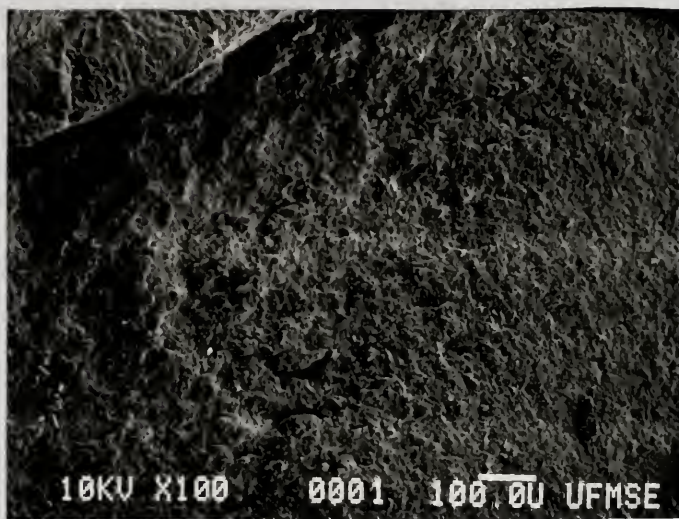


Figure 38. SEM Micrographs of PS252.

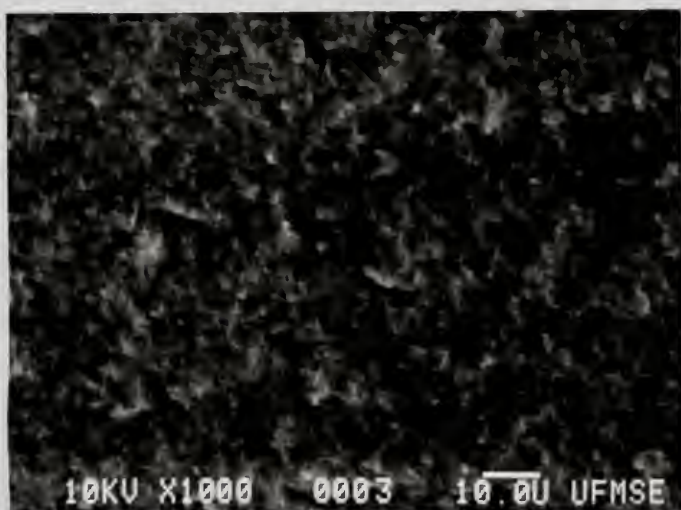


Figure 39. SEM Micrographs of PS2508.

volume fractions appearing in the figures previously described are nominal values, and thus Tables 5 and 6 should be consulted to determine the true respective composite filler concentration. The activation energies for the onset of viscous flow were calculated for most of the samples, and these results are given in Tables 7 and 8. Tables 9 through 12 contain the listings of the various model parameters that were obtained from the Adams model fits to both complex viscosity and reduced storage modulus data. Finally, an indication of the quality of the compounding performed is evidenced from the intrinsic viscosity data obtained from post compounded samples given in Table 13, and Table 14 displays the residual moisture remaining in the various size CaCO_3 fillers after vacuum drying.

Table 5. Actual Volume Fractions of CaCO_3 Filled Materials
(Determined from ashing).

<u>Sample ID</u>	<u>Nominal Volume Fraction</u>	<u>Measured Weight Fraction</u>	<u>Actual Volume Fraction</u>
PS520	0.05	0.118	0.047
PS1020	0.10	0.225	0.097
PS1520	0.15	0.309	0.142
PS2020	0.20	0.386	0.189
PS2520	0.25	0.46	0.24
PS0252	0.025	0.062	0.024
PS52	0.05	0.122	0.049
PS102	0.10	0.227	0.098
PS152	0.15	0.315	0.146
PS202	0.20	0.446	0.229
PS252	0.25	0.458	0.238
PS508	0.05	0.12	0.048
PS1008	0.10	0.221	0.095
PS1508	0.15	0.252	0.111
PS2008	0.20	0.382	0.186
PS2508	0.25	0.475	0.251
PS202 (molded)	0.20	0.448	0.231
PS202 (scrap)	0.20	0.449	0.232

Table 6. Actual Volume Fractions of Bimodally Distributed CaCO_3 Filled Materials (Determined from ashing).

<u>Sample ID</u>	<u>Nominal Volume Fraction</u>	<u>Measured Weight Fraction</u>	<u>Actual Volume Fraction</u>
PS128020	0.12	0.258	0.114
PS126040	0.12	0.258	0.114
PS125050	0.12	0.261	0.116
PS124060	0.12	0.263	0.117
PS122080	0.12	0.258	0.114
PS208020	0.20	0.392	0.193
PS206040	0.20	0.395	0.195
PS205050	0.20	0.396	0.195
PS204060	0.20	0.392	0.193
PS202080	0.20	0.387	0.190

Table 7. The Activation Energy for the Onset of Viscous Flow for CaCO_3 Filled PS Materials.

<u>Sample ID</u>	<u>Frequency, rad/S.</u>	<u>Activation Energy, kcal/mol</u>
PS Resin and all	1	$18.9 \pm 1.5\%$
CaCO_3 Composites	10	$14.6 \pm 3.0\%$
Except as Noted	100	$9.1 \pm 5.0\%$
Below *		

*Samples excluded include: PS2008, PS2508, PS202080, and PS204060

Table 8. The Activation Energy for the Onset of Viscous Flow for Rubber Filled PS Materials.

<u>Sample ID</u>	<u>Frequency, rad/S.</u>	<u>Activation Energy, kcal/mol</u>
HIPS500	100	9.3
	1	23.3
HIPS1000	10	13.3
	100	8.2
	1	20.9
HIPS1500	10	11.8
	100	6.6
	10	10.8
HIPS2000	10	5.9
	1	16.6
HIPS2500	10	9.4
	100	5.1

Table 9. Viscosity Model Parameters for CaCO_3 Filled PS Materials.

Sample ID	$\ln \eta_0^*$	$\ln \mu$	σ	s
PS Resin	8.32	1.7	1.9	-0.64
PS520	8.30	1.8	1.9	-0.67
PS1020	8.36	1.9	1.9	-0.66
PS1520	8.56	1.9	1.85	-0.68
PS2020	8.92	1.6	2.2	-0.63
PS2520	9.15	1.5	2.0	-0.60
PS0252	8.33	1.7	2.0	-0.62
PS52	8.47	1.8	2.0	-0.68
PS102	8.69	1.7	2.0	-0.68
PS202	9.02	1.7	1.9	-0.60
PS252	11.51	-0.62	3.7	-0.65
PS508	8.30	2.0	1.8	-0.69
PS1008	8.84	1.5	2.1	-0.62
PS1508	9.41	0.9	2.5	-0.63
PS2008	10.57	0.3	3.0	-0.65

Table 10. Viscosity Model Parameters for Rubber Filled PS Materials.

Sample ID	$\ln \eta_0^*$	$\ln \mu$	σ	s
PS Resin	8.32	1.7	1.9	-0.64
HIPS500	8.52	1.8	2.0	-0.72
HIPS1000	8.70	1.8	2.0	-0.75
HIPS1500	9.11	1.4	2.1	-0.77
HIPS2000	9.51	1.2	2.4	-0.80
HIPS2500	10.02	0.3	2.4	-0.72

Table 11. Reduced Storage Modulus Model Parameters
for CaCO_3 Filled PS Materials.

Sample ID	$\ln(G'_{R,0})$	$\ln \mu'$	σ'	S'
PS Resin	7.74	0.67	2.3	-1.55
PS520	7.42	1.04	2.4	-1.62
PS1020	7.49	1.08	2.5	-1.61
PS1520	7.70	1.08	2.5	-1.63
PS2020	8.38	0.52	2.6	-1.54
PS2520	8.84	0.39	2.8	-1.55
PS0252	7.57	0.70	2.2	-1.54
PS52	7.87	0.85	2.5	-1.64
PS102	8.30	0.70	2.7	-1.64
PS202	8.50	0.62	2.6	-1.54
PS252	22.8	-7.3	8.6	-1.63
PS508	7.49	1.08	2.5	-1.63
PS1008	8.61	0.28	2.6	-1.54
PS1508	11.3	-0.84	4.3	-1.58.
PS2008	17.05	-3.89	6.7	-1.64

Table 12. Reduced Storage Modulus Model Parameters
for Rubber Filled PS Materials.

Sample ID	$\ln (G'_{R,0})$	$\ln \mu'$	σ'	S'
PS Resin	7.74	0.67	2.3	-1.55
HIPS500	7.97	1.00	2.6	-1.66
HIPS1000	8.25	0.90	2.5	-1.70
HIPS1500	9.15	0.41	2.6	-1.73
HIPS2000	10.21	0.14	3.0	-1.77
HIPS2500	11.47	-0.83	3.0	-1.70

Table 13. Intrinsic Viscosities of Selected PS Composites.

<u>Sample ID</u>	<u>Intrinsic Viscosity, dl/g</u>
PS Resin	0.89
PS 1508	0.90
PS2508	0.90

Table 14. Residual Water Adsorbed on CaCO_3 After
Vacuum Drying (Determined by ashing).

<u>Average Particle Size, microns</u>	<u>Percent Residual Moisture, Weight %</u>
0.8	0.5
2.0	0.5
20.0	0.1

DISCUSSION OF RESULTS

The rheological properties of PS composites were determined as functions of filler type, concentration, particle size, and particle size distribution at temperatures ranging from 210-260°C and over a wide range of frequency. The results were used to test models to describe the frequency dependence of both the complex viscosity and the reduced loss modulus for the unimodally distributed systems, and percolation theory was determined to be useful in qualitatively explaining the results.

The PS-rubber and PS-CaCO₃ composites covering concentration ranges of 2.5 to 30 volume % for both unimodal and bimodal particle size distributions of filler ranging in size from 0.8 to 20 microns were compounded. Intrinsic viscosities of the compounded samples of PS1508 and PS 2508 were determined, and the results indicated that the polymer suffered no degradation during the compounding. The SEM micrographs of the compression molded test samples revealed that the quality of dispersion was quite good, and the reproducibility of the rheological results indicated that composite uniformity was excellent. This fact was reinforced by the results of ashing experiments conducted on molded test samples and on material trimmed from the tooling of the loaded rheometer. A sample of the compression molded plaque of PS202 was ashed to determine the filler concentration. Another sample of the same material from the same plaque was loaded into the rheometer, the gap was adjusted

as previously outlined, and the extruded scrap material was collected and also ashed. After the rheological testing was completed, the test sample was also ashed. Final agreement on the concentration of filler in the three samples was within $\pm 0.7\%$, indicating that filler migration during the loading process (which would be the worst scenario) was not a problem. For the most part, the final composite compositions were comparable to the nominal target values, and the discrepancies that occurred did not adversely affect the overall target concentration range.

Most of the rheological data were obtained by using a Rheometrics RMS-800 mechanical spectrometer equipped with parallel disk geometry. The radii of the disks used were 12.5 and 25 mm, and no effects due to disk radius or gap distance were noticed. Since oxidative degradation of the polymer at elevated temperature was found to be a problem, all of the viscoelastic data were obtained by operating the rheometer with a nitrogen rich sample environment. Strain sweeps of the materials were conducted to determine each sample's linear viscoelastic region, and constant rate temperature sweeps at times up to 30 minutes were also conducted to ensure sample thermal stability was maintained during the normal experimental time span.

Rheology of Filled Polystyrene

The rheological behavior of the various PS composites investigated was found to be a complex function of filler type, concentration, particle size, and particle size distribution. These effects and the model results emphasizing these effects will be discussed together.

Effect of Concentration

As expected the rheological properties (η^* , G' / ω^2 and G'' / ω) all increased with increase in filler concentration irrespective of the filler type. The amount of increase in η^* was considerably greater at lower frequencies as has been reported in the literature and previously cited, while at higher frequencies, the flow curves for the various concentrations at constant particle size showed signs of convergence. Similar results were obtained for the effect of concentration on the frequency dependence of the reduced moduli. Also in general, the elastic effects, as determined from the components of the complex modulus, decreased as the concentration of filler was increased. This fact has been noted by several observers as explained by Metzner (68).

For each of the filler types and sizes tested, the viscosity flow curves gradually increased with an increase in filler concentration at levels below approximately 15 volume %. At approximately 16 volume %, percolation theory predicts the appearance of a macroscopic ordered structure in the system, and experimentally, the flow curves showed a corresponding substantial increase above that concentration level.

Prediction of the limiting frequency complex viscosity, η_0^* (obtained via the Adams model) was attempted by applying the percolation based model developed by Campbell and Forgacs (47). The model yielded a reasonable fit to the data for 20 micron CaCO_3 filler with a maximum packing fraction approaching close packed ($\phi = 0.74$). Reasonable results were also obtained for the rubber filled PS system by using $\phi_m = 0.524$, (the maximum packing fraction associated with simple cubic packing). However, as the CaCO_3 particle size was decreased, the model consistently predicted lower values for η_0^* as a function of filler concentration. Values below that of simple cubic packing ($\phi_n = 0.524$)

were required to yield even modest agreement. Utracki and Fisa (4) have claimed that maximum packing fractions for CaCO_3 filled polymers may be as low as 0.36, however without knowing these values a priori, the model testing simply becomes a curve fitting process. Similarly, by also changing the value of ϕ_c (to lower values), the model predictions can be improved, but again data to justify such a shift was not available. In all fairness to Campbell and Forgacs however, if their assumptions regarding non-interacting rigid fillers could somehow be relaxed, the tendency of a new model based on these concepts would be to lower values of ϕ_c .

Effect of Particle Size

The fact that the flow curves above ϕ_c showed a substantial increase with decreasing particle size and the fact that at smaller particles sizes, η_0^* could not be predicted by the suspension equation of Campbell and Forgacs indicated that the particle size of the filler (and more likely the surface area of the filler) had a substantial impact on the composite rheological behavior. The complex viscosity in the limiting frequency region for PS2520 was 80% greater than that for PS1520, but the complex viscosity at similar frequency for PS2508 was approximately 1.5 orders of magnitude greater than that of PS1508. The particle size of the filler has been reported to have no effect on the viscosity of filled thermoplastics (68), and only the limited work (12,13,14,15 and 27) previously discussed has shown any effects of particle size.

The Adams viscosity model parameters were correlated with the total surface area of the composite based on the specific surface area

reported by the CaCO_3 manufacturers. No data on the specific surface area of the 20 micron CaCO_3 was available from OMYA Inc., but the model parameters ($\ln \mu$ and σ) both showed marked dependence on filler surface area. The reduced complex viscosity ($\eta_{0\text{composite}}^*/\eta_{0\text{polymer}}^*$) and the model parameters displayed discrete jumps in values at specific surface areas (A_w , m^2/g composite) of 2.7-2.8. Below $A_w = 2.7$, the values of the model parameters remained fairly constant, and for engineering calculations the constant value assumption was valid.

The results also indicated that the increase in viscosity at $\phi > \phi_c$ was substantially enhanced by decrease in particle size. This suggests that the surface area of the clusters formed in composite systems has an additional effect over the volumetric effects predicted by percolation theory. This is probably due to the increased drag of the polymer on the increased surface area during relative flow.

Effect of Particle Size Distribution

The limited data reported in the literature (35,45) suggested that the viscosities of multimodal suspensions were lower than those of unimodally dispersed fillers at equivalent loadings. Such was not the case with the bimodal composite systems tested. Below ϕ_c , the ratio of 20:2 micron CaCO_3 had virtually no effect on the composite viscosity. At concentrations greater than ϕ_c significant differences in compositional ratio were observed. For distributions where the 20 micron CaCO_3 was 50% of the total filler or more, the bimodally distributed composite viscosity curves were between the unimodally distributed flow curves for 20 and 2 micron CaCO_3 filled composites. However, when the 2 micron filler became the dominant species a discrete increase in viscosity

occurred, and the viscosities for PS202080 and PS204060 were significantly greater, particularly at lower frequencies, than either PS202 or PS2020. There were no studies found in the literature with which to compare these results since no one has apparently studied multimodal systems where the smaller sized filler is the dominant species, and the author knows of no available theory, deterministic or stochastic, to date which can explain the synergistic phenomena.

Again, the concentration effects in the bimodal systems showed a similar increase in η^* as ϕ became greater than ϕ_c . These effects were also substantially increased by making the 2 micron CaCO_3 the dominant species. Similar results were obtained for the components of the complex modulus.

Effect of Filler Type

The effects of filler type on the rheological properties of PS composites were examined by using rubber filled PS over a concentration range of 6 to 30 volume %. The average rubber particle size was approximately 1.9 microns. The effects of concentration on the elastically filled materials was similar to the rigid materials in that at concentrations greater than ϕ_c , the viscosity showed a marked increase at lower frequency. However, the shift in the critical frequency, that frequency where the onset of non-Newtonian behavior began, was shifted more to lower frequencies as ϕ was increased. This resulted in a more severe convergence of the flow curves at higher frequency. Although only one rubber particle size was available, apparently the reduced modulus of the filler was significant in reducing the effect of particle size or viscosity. This is probably due to the filler's ability to

deform upon shearing. The rubber filled material at 24 volume % (1.9 avg. particle size) displayed flow behavior comparable to PS2520. Therefore it appears that the decreased modulus of the filler has the effect of lowering the composite viscosity compared to a composite loaded with equivalent sized rigid filler.

Effect of Temperature

Although most of the results discussed thus far have been for data obtained at 210°C, the rheological measurements were taken at 235 and 260°C also. All of the viscosity responses of the PS-CaCO₃ composites with increase in temperature were similar as evidenced by the fact that the activation energies, E_a , for the onset of viscous flow, for the CaCO₃ filled materials were essentially constant for a given frequency. The value of E_a for all of the PS-CaCO₃ composites except PS2508, PS2008, PS202080, and PS204060 were within agreement of better than 5% over the entire frequency range investigated. At 1.0 rad/s, E_a for all of the valid PS-CaCO₃ composites, was 18.9 kcal/mole \pm 1.5%. The literature value for polystyrene at zero shear rate was 22.6 kcal/mole (69). It was impossible to make any comparative conclusions since the limiting frequency was not obtained in all of the cases studied. The data at elevated temperatures for the excluded samples were not reproducible and were therefore not included in the analysis. The reasons for this remain a mystery. The HIPS composites were similarly analyzed, and the E_a decreased with increase in rubber concentration. However, no discernable correlation between E_a and ϕ was found.

Cox-Merz Approximation

Comparisons of the complex viscosities obtained using the RMS-800 were compared with the data obtained by Kelly (30) for the unimodal PS-CaCO₃ composites using an ICR. Excellent agreement between η^* and η were obtained from this analysis for all of the PS-CaCO₃ systems except PS2508, PS2008, and PS252. Interestingly, these three samples had total filler specific surface area values greater than 2.7-2.8 m²/g composite. Thus for engineering estimates, the Cox-Merz approximation appeared to be valid for composite systems over a significant range of filler particle size and concentration. At some critical point, apparently dependent on total filler surface area, the Cox-Merz approximation failed.

Rheological Models for Composite Systems

The viscosity shear rate model developed by Adams (64) was shown to be applicable to filled PS systems. The model was capable of predicting the frequency dependence of the complex viscosity for both rubber and CaCO₃ filled polystyrene at accuracies of $\pm 5\%$ or better for all of the composites modelled. The versatility of the model was evidenced by the fact that it was also capable of predicting the reduced loss modulus as a function of frequency to within $\pm 7\%$ of the observed values. Since the limiting slope in the fully developed power-law region of the G''/ω versus ω curves was not available for many cases, the model was not applied to this case, however since the model's ability to accurately predict data that fit the general shape of a viscosity flow curve has been established, if data were obtained at higher frequencies, the model would probably prove useful in correlating the G'' results as well.

The simplex routine employed required the input of the slope of the fully developed power-law region and a set of initial guesses for the remaining model parameters. For a given slope, several varied sets of "adjustable" input parameter initial guesses were used, and the final model parameter values always approached unique solutions provided the convergence criterion was met. The slope in the fully developed power-law region was determined by averaging the value obtained from the oscillatory experiments (if available) and the value obtained from capillary experiments performed by Kelly (30). The differences in values obtained by these methods resulted in negligible scatter in the predicted zero shear viscosity and in variations of no worse than $\pm 5\%$ for the other two parameters ($\ln \mu$ and σ).

Although no valid mathematical expressions for the various viscosity model parameters were obtained, two very useful results were discovered. First, although the available percolation model did not accurately predict η_0^* results, percolation theory was useful in predicting the change in η_0^* at ϕ approaching and surpassing ϕ_c . Secondly, the model parameters, and thus the viscosity, were shown to be significantly influenced by A_w , and the behavior below a "critical" value for A_w was apparently not significantly influenced by ϕ . The behavior above the "critical" A_w was shown to be dependent on the filler particle size. It should be noted that the ashing experiments conducted using samples PS252 and PS202 were replicated, and the actual filler concentrations were within $\pm 0.2\%$ or better. It should also be noted that η_0^* for PS2508 was unattainable either experimentally or by modelling, since the behavior the entire frequency range investigated was of a power-law nature. Attempts to extend the frequency range to lower frequencies for

PS2508 were unsuccessful. The resulting $\eta^* - \omega$ relationship remained linear but was not reproducible in three attempts. This may have been due to increased structure formation at lower frequencies, but the results were inconclusive.

Although the model was not successful at completely predicting the behavior over all experimental ranges of the variables, the utility of the model to obtain engineering estimates proved to be excellent. By assuming constant average values of the various model parameters below the apparent critical A_w and by using the results of the frequency dependence of E_A , the complex viscosity-frequency curves can be predicted to within $\pm 25\%$ over the entire temperature and frequency range investigated. The analysis is valid for volume fractions ≤ 0.2 and/or $A_w \leq 2.7 \text{ m}^2/\text{g}$ composite.

Phenomenological Interpretations

The viscosity of a fluid in general is related to the relaxation of the system when sheared. If the relaxation process is short, the viscosity is low, and if the relaxation process is longer, the viscosity increases. In polymers, the macromolecules exist as flexible chains in random coils (70). Deformation distorts the distribution of conformations, and the chains form new conformations. These are caused by the viscous forces from relative motions of their surroundings. Brownian motion tends to restore equilibrium, and the competition of these two effects determine the average distortion at any moment, and thus determines the stress. The characteristic relaxation time of a polymer, λ , is a measure of the system's ability to dissipate the energy added due to shearing.

It is speculated, using the percolation concepts previously reported, that the increase in limiting shear viscosity due to the addition of fillers may be attributed to the decrease in void sites in a statistical three dimensional lattice. It is hypothesized that at $\phi < \phi_c$, the filler exists as single particles and small groups of connected clusters randomly distributed. The fluid molecules move, in the voids available, relative to the filler particles. At low filler concentration, the filler particles can readily move to neighboring sites, thus leaving voids for the fluid particles to move into.

At $\phi < \phi_c$, voids are prevalent, and single particles and small clusters are able to move to empty sites. However as ϕ increases, the void fraction decreases, and thus the probability that a filler particle can find an empty site is reduced. As ϕ approaches ϕ_c , longer range order in the filled system develops. At ϕ_c , a macroscopic ("infinite") cluster of filler forms, and with this development, it becomes increasingly difficult to find available "holes" for the filler to move into. Additionally, since the structure exists in a connected entity, in order for one of the particles in the cluster to move into a hole, the remaining contacting particles must be moved accordingly. Since the cluster is not moving as readily into and out of the fewer available holes, the fluid molecules find it increasingly difficult to find voids (either existing or vacated by cluster particles) to move into, and hence the relaxation time of the system increases more rapidly. Therefore at ϕ slightly greater than ϕ_c , the viscosity of the system begins to increase more rapidly with the further addition of filler particles.

As ϕ continues to increase, secondary structure formation occurs, and thus the probability of finding available holes rapidly decreases.

The three dimensional cluster becomes increasingly difficult to rearrange, and thus the molecular motions of the fluid molecules become further restricted. If the surface area of the rigid structured system is high (due to lower particle size), the increased molecular friction attributed to the relative flow enhances the observed viscosity increase. Similarly, if the filler particles are interacting (as in real systems) for example by collisions, the system is capable of additional energy dissipation, and the viscosity of the composite is increased. As ϕ approaches ϕ_m , the macroscopic cluster cannot be rearranged and thus cannot move into and out of the decreased available holes. Thus at $\phi = \phi_m$, the system viscosity approaches infinity.

In a shear field and at sufficiently low deformation rate, the viscosity of a fluid system (filled or unfilled) equals the limiting shear viscosity, η_0 . In this range of deformation rate, large molecules (as in high molecular weight polymeric systems) can deform quickly enough to move segments of their chain structure into and out of available holes in the system and dissipate energy through molecular friction. As $\dot{\gamma}$ (or ω) increases, the largest molecules become trapped in certain configurations in the melt and cannot move into and out of the available holes fast enough, and therefore cannot dissipate energy as effectively. This is the onset of non-Newtonian flow. Further increases in $\dot{\gamma}$ trap more and more molecules until only the smallest molecules are able to deform rapidly enough to effectively dissipate energy, and the viscosity further decreases.

The addition of rigid filler particles to the system effectively removes some of the available void space in the system as previously discussed. Now, in order for the large molecules to be able to deform

quickly at a given deformation rate, their motions are dependent upon the coordinated movement of the filler particles into available holes. The result is that the zero shear viscosity region of filled systems is shifted to lower deformation rates as the concentration of filler is increased, and the onset of non-Newtonian flow also occurs at lower rates of deformation.

Since elasticity in polymer melts is manifested at the local segment level, the relaxation time attributed to elastic recovery is very low and is probably a small contribution to λ for the entire molecular rearrangement of the system. The elastic properties of the polymer in filled systems are related to the reduction in available configurations allowed with increase in filler concentration. Thus as ϕ increases, the influence of elastic effects decreases.

Limitations of Results

The accuracy of the viscosity results obtained using the RMS-800 were determined from standard dead weight testing as outlined by the manufacturer. From Table 15 it can be seen that for torque scale readings less than 10% of scale, the error increased non-linearly, and therefore only viscosity data at torque values greater than or equal to 10% of scale were accepted as valid. Since the torque was used to calculate G' and G'' , the same accuracies applied.

The dynamic oscillatory experiments were conducted for each sample at each temperature over a frequency range of at least 0.1 to 100 rad/s. Typically, the dynamic experiments were replicated at least once for each disk (12.5 and 25 mm radii respectively) used. Normal

Table 15. Torque Calibration Data for RMS-800
with 2000 g-cm Transducer.

<u>Dead Weight Applied, g</u>	<u>Actual Torque, g-cm</u>	<u>RMS-800 Torque Reading, g-cm</u>	<u>Error, %</u>
0	0	0.35	---
0.2	1.0	0.762	23.8
0.5	2.5	2.14	13.6
1	5.0	4.48	10.4
10	50	49.48	1.04
50	250	249	0.40
100	500	499.6	0.08
200	1000	999 \pm 0.5	0.10

operation involved using the 25 mm tooling to generate rheological data over a frequency range of 0.1 to 10 rad/s and then using the 12.5 mm tooling to collect data over a frequency range of 10 to 100 rad/s. Each of these experiments was replicated at least once, yielding one replication of rheological data in the ranges $0.1 \leq \omega < 1.0$ and $10 < \omega \leq 100$ and three replications of the rheological data in the $1 \leq \omega \leq 10$ range. The standard deviations of the rheological data were not calculated since for the typical experiment, the number of replications varied with the frequency as described above. However the reproducibilities, or in other words, the precision of η^* was determined for each flow curve by using the total variation about the mean value at the data point with greatest variability to be $\pm 5-7\%$ for $\phi \leq 20$ volume % and $\pm 8-10\%$ for $\phi = 25$ volume %. The modulus data showed somewhat greater variation with precisions of $\pm 5-10\%$ for $\phi \leq 20$ volume % and $\pm 10-20\%$ for $\phi = 25$ volume %. These precisions which represent worst cases were quite acceptable considering the complex nature of the sample and the fact that temperature control of the set point temperature was $\pm 1^\circ\text{C}$.

Attempts to extend the complex viscosity curves for PS252 and PS2508 to lower frequencies were unsuccessful. At frequencies ranging from 10^{-2} to 10^{-1} the rheological data were not reproducible and thus were not included. The time required to measure the rheological properties at these low frequencies may have been sufficiently large to allow additional structure to be established in the system. Variable structure formation could possibly explain the variations observed in the measured properties. The time required to obtain low frequency data ($\omega = 10^{-3}$ to 10^{-1} rad/s range) was estimated to be 3.25 hours per experiment. This time scale was considered to be much too large due to both thermal degradation and excessive liquid nitrogen costs.

An additional unexplained anomaly was observed during the experiments conducted using PS152. At each tool radius, the flow curves were replicated twice, the flow curves at $0.1 \leq \omega \leq 10$ and at $10 \leq \omega \leq 100$ were reproduced to within $\pm 3-5\%$. However, at the frequency range ($1 \leq \omega \leq 10$) common to each experiment the variation in complex viscosity was 25-30%. The reasons for this were never confirmed.

The model predictions of the complex viscosity were better than $\pm 3\%$ for all of the samples modelled, and the corresponding G'/ω^2 model predictions were all within $\pm 5\%$ of the actual data. Variations in initial guesses for the model parameters in the simplex routine had no effect on the final values of the model parameters upon convergence.

Some of the actual volume fractions of the composites varied from the target values (PS202 e.g.). The ashing experiments were duplicated, and the calculated volume fractions were within $\pm 0.2\%$ of their corresponding replicates. Thus the variations in actual versus target processing concentrations were considered statistically valid, and although the legends used in the figures represent the nominal target values, the actual concentrations were used throughout the analysis.

CONCLUSIONS

The investigation of the rheological properties of various PS composites was conducted according to the previously described experimental plan, and the results of the study led to the following conclusions:

1. The viscoelastic properties (η^* , G' , and G'') of both CaCO_3 and rubber filled polystyrene composites were dramatically affected by not only the filler concentrations, but also the filler type, filler particle size, and filler particle size distribution.
2. The rheological properties were significantly influenced by the total specific surface area of the respective composite. The parameters used in the Adams model displayed discontinuity at an apparent critical value of the filler specific surface area. The critical value of A_w was determined to be $2.7 \text{ m}^2/\text{g}$ of composite irrespective of the particle size, and that value was only obtained for samples with $0.12 \leq \phi \leq 0.22$. The concentration range corresponded well with the theoretical value of the critical percolation concentration ($\phi_c = 0.16$).
3. A solute-solvent based viscosity model for polymer melts successfully predicted the frequency dependence of both the composite complex viscosity and the composite reduced loss modulus.

4. Percolation theory was found to be useful in semi-quantitatively describing the rheological behavior of the composite systems. Additionally, a stochastic slurry viscosity model based on percolation concepts was tested and was shown to be capable of qualitatively predicting the filler concentration dependence of the limiting frequency viscosity behavior of rubber filled and $20\text{ }\mu\text{m CaCO}_3$ filled polystyrene composites. As the CaCO_3 particle size was decreased, the model failed to predict the observed behavior.
5. The Cox-Merz approximation was valid in relating the complex viscosity to the steady shear viscosity for most of the composite systems. The approximation failed to yield engineering estimates for PS2508, PS2008, and PS252, each of which had total specific filler surface areas greater than $2.7\text{ m}^2/\text{g}$ of composite.

RECOMMENDATIONS

As the investigation progressed, it was realized that modifications to the experimental plan and further investigation of the various composite systems would be necessary. Therefore, the following recommendations were suggested to expand the knowledge base obtained from this study.

1. Obtain valid lower frequency data to determine η_0^* for the highly filled materials containing smaller particle size fillers. This may possibly be accomplished by obtaining enough low frequency and low shear rate data to prove the validity of the Cox-Merz approximation. If the approximation holds at low deformation rate, the remaining data may be obtained via steady shear operation which would reduce the experimental time.
2. Further investigate the effects of lower temperatures on the rheological properties of the PS composites. Quantify the relationship between temperature and viscosity for highly filled systems containing small particle size fillers.
3. Use the results of this investigation to design and implement a better experimental plan to determine both the effects of filler surface area and the relationship between percolation theory and rheological properties of composite systems.

It is recommended that this investigation be continued in order to accomplish the first two goals. Simultaneously, a second study should be initiated using spherical, and even better, conducting spherical fillers, with concentration and particle size ranges suggested by these results, to help quantify the effects of filler surface area and the application of percolation theory to heterophase polymer systems. By using conducting fillers, the rheological measurements can be supplemented with conductivity measurements to try to determine the filler level at which a conducting network through the system (ϕ_c) is formed.

APPENDIX



OMYA, INC.

61 Main Street
Proctor, Vermont 05765
Tel (802) 459-3311
Telex 95 46 28 OMYA PRTR

OMYACARB'UF

OMYACARB'UF is a high purity, ultrafine, wet ground natural Calcium Carbonate available in dry or slurry form.

Paint Applications

OMYACARB'UF is a spacing extender that facilitates the conversion from latex grade to enamel grade titanium dioxide with dramatic cost reductions in interior latex flats.

It may be used in water based and solvent based flat, low sheen, semi-gloss and high-gloss systems

Higher and sharper gloss with whiter whites and cleaner pastels are obtainable in eggshell, semi-gloss and gloss finishes

OMYACARB'UF works well in conjunction with the newer opacifying polymers and beads.

Typical Dry Properties

Refractive Index	1.57
Dry Brightness (Green Filter)	95
DOP-PASTE Brightness	
Blue Filter	64
Pounds Pigment/Solid Gallon	22.6
Oil Absorption	19 ± 1
g of Oil/100 g Pigment	
(rub-out method, ASTM D 281-31)	
DOP Absorption	29 ± 1
g of DOP/100 g Pigment	
(rub-out method, ASTM D 281-31)	
Moisture Loss at 110°C (%)	0.25
Specific Gravity	2.7
Apparent Bulk Density g/cc	
Loose	0.45
Packed	0.65
Hegman Grind	5.5

Typical Slurry Properties

Solids as Supplied (%)	76
Specific Gravity	1.93
Slurry Density (lbs./gal.)	16.05
Pounds Pigment/Gallon	12.2
Brookfield Viscosity (cps)	
(#3 Spindle, 100 rpm)	200 ± 100
Hegman Grind	5.5
pH Slurry	9.4 ± 0.3

Particle Size

Top Cut	4 Microns
% Finer than 2 Microns	90
% Finer than 1 Micron	65
Specific Surface Area (m ² /g)	12

Typical Chemical Analysis

CaCO ₃ (%)	98
MgCO ₃ (%)	less than 1.0
Acid Insoluble (%)	less than 0.5

Plastic Applications

OMYACARB'UF offers higher impact properties at higher loading levels than are available utilizing coarser grades

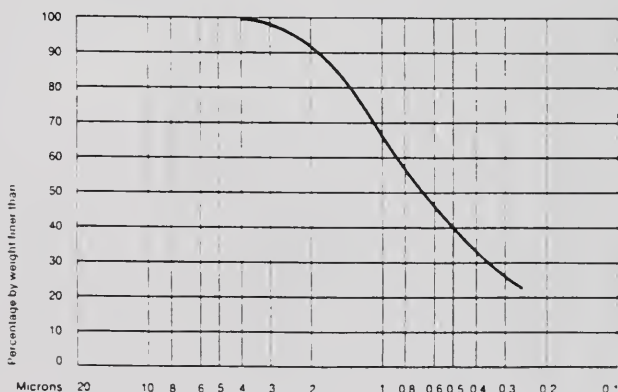
The low top cut and mean particle size as well as near absence of impurities significantly reduce abrasion in mixers and extruders.

Flexible PVC	Rigid PVC
Calendered	Pipe
Wire & Cable	Fittings
	Profile

Regulatory Approvals (Food Chemical Codex)

OMYACARB'UF is FDA approved for use in thermoplastics for food contact and under FDA 21CFR Sections 175.105, 175.300, 176.170, 176.180 and 177.1210

Typical particle size distribution curve



Other than a representation that the products sold by OMYA are of the average, mean or criteria set forth above, which is and shall be subject to confirmation by the purchaser, OMYA makes no warranty, guarantee or representation of any kind, express or implied, and specifically EXCLUDES any and all WARRANTIES OF MERCHANTABILITY AND FITNESS FOR A PARTICULAR PURPOSE. OMYA makes no other warranties beyond those contained herein and in any of the products. In any event, it is the purchaser's sole responsibility to provide notice to OMYA of such non-conforming product. Such notice shall be given within fourteen (14) days of delivery, and OMYA will, at its option and if it determines the product does not conform, either promptly replace the non-conforming product or refund the purchase price paid for the non-conforming product. In no event shall OMYA be liable for special, indirect or consequential damages nor shall OMYA be liable for damages of any kind arising from the purchase or use of the products, whether used singly or in combination with other substances. OMYA disclaims any liability arising from use of the products which may infringe upon patents, trademarks or pending or existing, no claim of any kind arising hereunder shall be greater than that which OMYA is in any event liable for an amount in excess of the amount of purchase price of the products in respect of which such claim is made.

VERMONT
(802) 459-3311
TLX 954628 OMYA PRTR

CALIFORNIA
(619) 248-7306
TLX WU 67-6344

 A PLEUSS-STAUFFER COMPANY

INDUSTRIAL FILLERS LTD.

2020 University Street
Suite 1255
Montreal, Canada H3A 2A5
Tel (514) 844-3425

PULPRO 20

Typical Physical Properties

Dry Brightness (Green Filter)	87
Refraction Index	1.60
Specific Gravity	2.71
Oil Absorption	7.5

(Rub-out Method ASTM D281-31)

pH Saturated Solution	< 10
Moisture Loss at 110°C (%)	< 0.5

Apparent Bulk Density
Loose Bulk Density 1 gram/cc

Packed Bulk Density	1.43 gram/cc or 62 lbs/ft ³
---------------------	-------------------------------------------

Packed Bulk Density 1.43 gram/cc
or 82 lbs/ft³

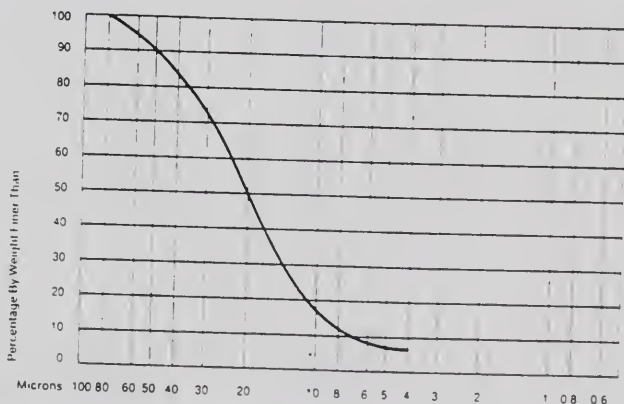
Typical Particle Size

% Retained on 325	10
Top Cut	80 microns
Mean Particle Size	20 microns

Typical Chemical Analysis

CaCO ₃ (%)	96
MgCO ₃ (%)	< 2
Acid insolubles (%)	< 4

Typical Particle Size Distribution Curve

[illegible]



OMYA, INC.

61 Main Street
Proctor, Vermont 05765
Tel: (802) 459-3311
Telex: 95 46 28 OMYA PRTR

OMYACARB[®]F

OMYACARB[®]F is a high purity fine, wet ground natural Calcium Carbonate available in dry or slurry form. Typical applications are:

Paint Applications

Water based and solvent based flat, low sheen and semi-gloss systems.

Formulating clean whites and pastels is enhanced by the clean top cut uniformly fine particle size, high calcium carbonate content and exceptional brightness of OMYACARB[®]F.

Contribution to flow and leveling is supplied by the Rhombohedral particle shape.

Plastic Applications

OMYACARB[®]F is generally the product of choice in Calendered PVC. It may be used in Rigid PVC where the better dispersion and higher loading potential of surface treated OMYACARB[®] FT or OMYACARB[®] UFT are not required. May also be used in Polyolefins although the surface treated products are normally preferred.

Flexible PVC Rigid PVC
 Calendered Profile
 Wire and Cable Pipe

Polyolefins
 Polyethylenes (LD, LLD, HD)
 Polypropylene
 Polystyrene

Regulatory Approvals (Food Chemical Codex)

OMYACARB[®]F is FDA approved for use in thermoplastics for food contact and under FDA 21CFR Sections 175.105, 175.300, 176.170, 176.180 and 177.1210.

Typical Dry Properties

Refractive Index	1.57
Dry Brightness (Green Filter)	95
DOP-PASTE Brightness	
Blue Filter	64
Pounds Pigment/Solid Gallon	22.6
Oil Absorption	17 ± 1
g of Oil/100 g Pigment	
(rub-out method, ASTM D 281-31)	
DOP Absorption	27 ± 1
g of DOP/100 g Pigment	
(rub-out method, ASTM D 281-31)	
Moisture Loss at 110°C (%)	0.15
Specific Gravity	2.7
Apparent Bulk Density g/cc	
Loose	0.55
Packed	0.75
Hegman Grind	5.5

Typical Slurry Properties

Solids as Supplied (%)	72 ± 1
Specific Gravity	1.84
Slurry Density (lbs./gal.)	15.31
Pounds Pigment/Gallon	11.0
Brookfield Viscosity (cps)	
(#3 Spindle, 100 rpm)	200 ± 100
Hegman Grind	5.5
pH Slurry	9.4 ± 0.3

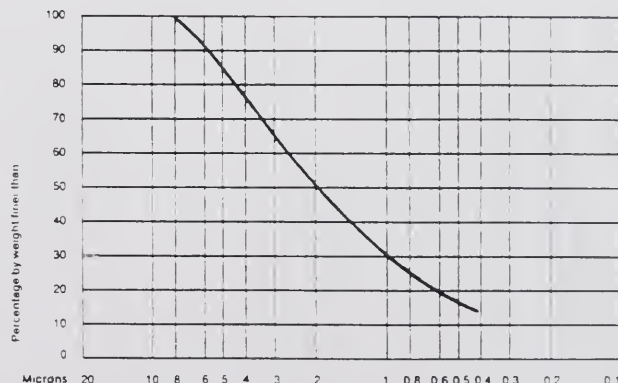
Particle Size

Top Cut	8 Microns
% Finer than 2 Microns	50
% Finer than 1 Micron	30
Specific Surface Area (m ² /g)	6

Typical Chemical Analysis

CaCO ₃ (%)	98
MgCO ₃ (%)	less than 1.0
Acid Insoluble (%)	less than 0.5

Typical particle size distribution curve



Other than a representation that the products sold by OMYA are, on the average, near the criteria set forth above, which is and shall be subject to confirmation by the purchaser, OMYA makes no warranty, guaranty or representation of any kind and expressly or impliedly EXCLUDES any and all WARRANTIES OF MERCHANTABILITY AND FITNESS FOR A PARTICULAR PURPOSE. OMYA makes no other warranties beyond those contained herein and in any of the products in any amount. It is the responsibility of the purchaser to determine whether the products sold by OMYA are suitable for the intended use. OMYA makes no warranty, guaranty or representation of any kind and expressly or impliedly EXCLUDES any and all WARRANTIES OF MERCHANTABILITY AND FITNESS FOR A PARTICULAR PURPOSE. OMYA makes no other warranties beyond those contained herein and in any of the products in any amount. It is the responsibility of the purchaser to determine whether the products sold by OMYA are suitable for the intended use.

VERMONT
(802) 459-3311
TELEX 954628 OMYA PRTR

CALIFORNIA
(619) 248-7306
TELEX 954628 OMYA PRTR



A PRINCE-EDLIER COMPANY

REFERENCES

1. R.J. Martino, ed., Modern Plastics, 65(1), 63 (1988).
2. R. Leaversuch, Modern Plastics, 65(5), 53 (1988).
3. R.B. Bird, R.C. Armstrong and O. Hassager, "Dynamics of Polymeric Liquids," Vol. 1, John Wiley & Sons, New York (1977).
4. L.A. Utracki and B. Fisa, Poly. Comp., 5(4), 277 (1984).
5. J. Ritter, Appl. Poly. Symp. No. 15, 239 (1971).
6. N. Minagawa and J.L. White, J. Appl. Poly. Sci., 20, 501 (1976).
7. A.J. Poslinski, M.E. Ryan, R.K. Gupta, S.G. Seshadri and F.J. Frechette, ANTEC, 41, 700 (1986).
8. T.G.M. Van de Ven, Poly. Comp., 6(4), 209 (1985).
9. C.D. Han, J. Appl. Poly. Sci., 18, 821 (1974).
10. B.A. Knutsson, J.L. White and K.B. Abbas, Proc. of the Int'l. Congress on Rheology 8th, 3, 83 (1972).
11. D.R. Saini and A.V. Shenoy, Poly. Engr. Sci., 26(6), 441 (1986).
12. F.M. Chapman and T.S. Lee, SPE Journal, 26, 37 (1970).
13. T. Kitano, T. Kataoka, T. Nishimura and T. Sakai, Rheol. Acta, 19, 764 (1980).
14. T. Kataoka, T. Kitano, M. Sasahara and K. Nishimura, Rheol. Acta, 17, 140 (1978).
15. T. Kataoka, T. Kitano, Y. Oyanagi and M. Sasahara, Rheol. Acta, 18, 635 (1979).
16. T. Kitano, T. Nishimura, T. Kataoka and T. Sakai, Rheol. Acta, 19, 671 (1980).
17. R.E.S. Bretas and R.L. Powell, Rheol. Acta, 24, 69 (1985).
18. D.M. Bigg, Poly. Engr. Sci., 23(4), 206 (1983).
19. D.M. Bigg, Poly. Engr. Sci., 22(8), 512 (1982).

20. J.E. Stamhuis and J.P.A. Loppe, Rheol. Acta, 21, 103 (1982).
21. A.M. Zolotor, Modern Plastics, 47(12), 68 (1970).
22. S.N. Maiti and P.K. Mahapatro, Poly. Comp., 9(4), 291 (1988).
23. F. Danusso, G. Tieghi and A. Lestingi, J. Appl. Poly. Sci., 33, 2137 (1987).
24. L.A. Utracki, B.D. Favis and B. Fisa, Poly. Comp., 5(4), 277 (1984).
25. N.J. Mills, J. Appl. Poly. Sci., 15, 2791 (1971).
26. B. Fisa and L.A. Utracki, Poly. Comp., 5(1), 36 (1984).
27. Y. Suetsugu and J.L. White, J. Appl. Poly. Sci., 28, 1481 (1983).
28. B. Hinkelmann and G. Mennig, Chem. Eng. Commun., 36, 211 (1985).
29. E. Sideridis, Comp. Sci. and Tech., 27, 305 (1986).
30. J.S. Chong, E.B. Christiansen and A.D. Baer, J. Appl. Poly. Sci., 15, 2007 (1971).
31. Y. Suetsugu and J.L. White, J. Non-Newt. Fl. Mech., 14, 121 (1984).
32. A.V. Shenoy and D.R. Saini, J. Reinf. Plast. and Comp., 5, 62 (1986).
33. F. Nazem and C.T. Hill, Trans. Soc. Rheol., 18(1), 87 (1974).
34. P.K. Agarwal, E.B. Bagley and C.T. Hill, Poly. Eng. Sci., 18(4), 282 (1978).
35. R.J. Farris, Trans. Soc. Rheol., 12(2), 281 (1968).
36. A. Vaxman, M. Narkis, A. Siegmann and S. Kenig, J. Mat. Sci. Let., 7, 25 (1988).
37. H.M. Laun, Coll. Poly. Sci., 262, 257 (1984).
38. B.A. Knutsson, J.L. White and K.B. Abbas, J. Appl. Poly. Sci., 26, 2347 (1981).
39. Y. Chan, J.L. White and Y. Oyanagi, J. Rheol., 22(5), 507 (1978).
40. G. Akay, Poly. Eng. Sci., 22(16), 1027 (1982).
41. R.J. Crowson and M.J. Folkes, Poly. Eng. Sci., 20(14), 934 (1980).
42. R.J. Crowson, M.J. Folkes and P.F. Bright, Poly. Eng. Sci., 20(14), 925 (1980).

43. R.J. Crowson, A.J. Scott and D.W. Saunders, Poly. Eng. Sci., 21(12), 748 (1981).
44. B. Chung and C. Cohen, Poly. Eng. Sci., 25(16), 1001 (1985).
45. J.L. White and J.W. Crowder, J. Appl. Poly. Sci., 18, 1003 (1974).
46. D. Stauffer, "Introduction to Percolation Theory," Taylor and Francis, Philadelphia (1985).
47. G.A. Campbell and G. Forgacs, in preparation (1989).
48. G. Mackay and N. Jan, J. Phys. A, 17, L757 (1981).
49. P.G. de Gennes, La Recherche, 7, 919 (1976).
50. J. Webman, J. Jorther and M.H. Cohen, Phys. Rev. B, 11, 2885 (1975).
51. P.J. Flory, J. Am. Chem. Soc., 63, 3091 (1941).
52. W. Stockmayer, J. Chem. Phys., 11, 45 (1943).
53. Y. Termonia and S. Reich, Phys. Lett., 111A, 138 (1985).
54. X. Quan, J. Poly. Sci.: Part B: Poly. Phys., 25, 1557 (1987).
55. H. Scher and R. Zallen, J. Chem. Phys., 53, 3759 (1970).
56. M. Borkovee, H. Eicke, H. Hammerich and B.D. Gupta, J. Phys. Chem., 92, 206 (1988).
57. R.F. Berg, M.R. Moldover and J.S. Huang, J. Chem. Phys., 87(6), 3687 (1987).
58. J. Peyrelasse, M. Moha-Ouchane and C. Boned, Phys. Rev. B, 38(8), 4155 (1988).
59. D.M. Heyes, J. Non-Newt. Fl. Mech., 27, 47 (1988).
60. A. Einstein, Ann. Physik, 17, 549 (1905).
61. H.L. Frisch and R. Simha in "Rheology," F.R. Eirich, ed., Ch. 14, Academic Press, New York (1956).
62. H. Brenner, Progr. Heat Mass Transfer, 5, 89 (1972).
63. T. Farrington, Ph.D. Dissertation, University of Maine, Orono, ME (1985).
64. M.E. Adams, M.S. Thesis, Clarkson University, Potsdam, NY (1987).
65. P.C. Hiemenz, "Polymer Chemistry," Marcel Dekker, Inc., New York (1984).

66. W.P. Cox and E.H. Merz, J. Poly. Sci., 28(18), 619 (1958).
67. J. Kelly, M.S. Thesis, University of Florida, Gainesville, FL (1989).
68. A.B. Metzner, J. Rheol., 29(6), 739 (1985).
69. M.L. Miller, "The Structure of Polymers," Reinhold Corp., New York (1966).
70. W.W. Graessley, Adv. Poly. Sci., 16, 7 (1974).

BIOGRAPHICAL SKETCH

The author was born in Charleston, SC, on January 17, 1958, and attended the public schools in the James Island district. He attended Fort Johnson High School from August, 1972, until his graduation in June, 1976.

In August, 1976, he entered Clemson University to pursue a degree in chemical engineering. From May, 1977, through May, 1980, he participated in the Cooperative Education Program, working alternate semesters at the Westvaco Corporation's Charleston, SC, facilities. He received his B.S. in chemical engineering in May, 1981.

Following graduation, he joined the Technical Department of Westvaco's Kraft Division in Charleston, SC, where he worked until taking a leave of absence in August, 1982, to pursue graduate studies. In September, 1982, he entered the Chemical Engineering Department at the University of Maine at Orono as a graduate research assistant in Professor Arthur L. Fricke's Black Liquor Physical Properties research program. In December, 1984, he received his M.S. degree in chemical engineering from UMO.

After completing the M.S. degree, the author transferred to the University of Florida in January, 1985, to continue working with Professor Fricke in the Department of Chemical Engineering. The author continued to work on the Black Liquor Physical Properties Project, while conducting research in the area of polymer composite rheology. In

December, 1988, the author accepted a position with Eastman Kodak in the Chemical Division's Performance Plastics Research Group in Kingsport, TN, while completing his dissertation. During that time he remained a part-time graduate student at the University of Florida where he is currently a candidate for the degree of Doctor of Philosophy in chemical engineering.

I certify that I have read this study and that in my opinion it conforms to acceptable standards of scholarly presentation and is fully adequate, in scope and quality, as a dissertation for the degree of Doctor of Philosophy.



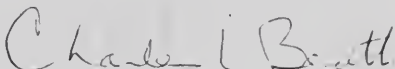
Arthur L. Fricke, Chairman
Professor of Chemical Engineering

I certify that I have read this study and that in my opinion it conforms to acceptable standards of scholarly presentation and is fully adequate, in scope and quality, as a dissertation for the degree of Doctor of Philosophy.



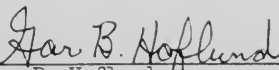
Murat O. Balaban
Assistant Professor of Food
Science and Human Nutrition

I certify that I have read this study and that in my opinion it conforms to acceptable standards of scholarly presentation and is fully adequate, in scope and quality, as a dissertation for the degree of Doctor of Philosophy.



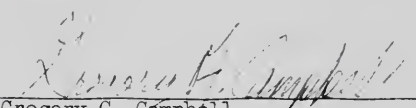
Charles L. Beatty
Professor of Materials Science and
Engineering

I certify that I have read this study and that in my opinion it conforms to acceptable standards of scholarly presentation and is fully adequate, in scope and quality, as a dissertation for the degree of Doctor of Philosophy.



Gar B. Hoflund
Professor of Chemical Engineering

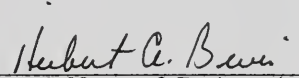
I certify that I have read this study and that in my opinion it conforms to acceptable standards of scholarly presentation and is fully adequate, in scope and quality, as a dissertation for the degree of Doctor of Philosophy.



Gregory C. Campbell
Associate Professor of Chemical
Engineering, Clarkson University,
Potsdam, NY

This dissertation was submitted to the Graduate Faculty of the College of Engineering and to the Graduate School and was accepted as partial fulfillment of the requirements for the degree of Doctor of Philosophy.

May 1989



Dean, College of Engineering

Dean, Graduate School

